Geological Society of America
Special Paper 388
2005

Hotspots: A view from the swells

John E. DeLaughter**
ChevronTexaco Exploration Production Co. Houston, Texas 77002, USA
Carol A. Stein*
Department of Earth and Environmental Sciences, University of Illinois at Chicago, Chicago, Illinois 60607-7059, USA
Seth Stein
Department of Geological Sciences, Northwestern University, Evanston, Illinois 60208, USA

The central problem is satisfactorily defining normal.
Menard (1969)

ABSTRACT

The magnitude of inferred depth and heatflow "anomalies" at hotspot swells relative to "normal" seafloor plays a major role in constraining the causes of these swells. Hotspot heatflow anomalies were first believed to be large and consistent with the uplift expected from thermal thinning of the lower lithosphere. However, these anomalies were overestimated because reference thermal models predicted greater depths and lower heat-flow than was typical of lithosphere older than 70 Ma. In contrast, models GDH1 and GDH2, derived by joint fitting of heatflow and bathymetry (and geoid slope for the latter) yield a hotter and thinner lithosphere than previous models and fit depth, heatflow, and geoid data significantly better. Hence heatflow on the Hawaiian and other swells is at most slightly high relative to GDH1 and GDH2. The absence of a significant heatflow anomaly favors a primarily dynamic or compositional rather than thermal swell origin. Similarly, the depths and heatflow for the Darwin rise are consistent with thin-plate models, and thus it is not thermally different from lithosphere of similar age. In younger lithosphere, where observed heatflow is less than that predicted from conduction-only models, the observed heatflow at hotspots can be compared to its global average. The heatflow for the south Pacific superswell is consistent with unperturbed lithosphere, and hence excludes significant lithospheric thermal thinning. Near Iceland, heatflow west of the Mid-Atlantic Ridge is consistent with the global average, but to the east is higher, the opposite of that predicted by models that involve an eastward-migrating plume.

Keywords: heatflow, depth, hotspot, mantle plume, lithosphere

*E-mail: cstein@uic.edu.
**Current address: EarthScope, 1200 New York Avenue, NW, Suite 700, Washington, D.C., 20005.

DeLaughter, J.E., Stein, C.A., and Stein, S., 2005, Hotspots: A view from the swells, *in* Foulger, G.R., Natland, J.H., Presnall, D.C., and Anderson, D.L., eds., Plates, plumes, and paradigms: Geological Society of America Special Paper 388, p. 257–278.

INTRODUCTION

The steady increase in ocean depth away from mid-ocean ridges provides our strongest constraint on the physics of the plate tectonic cycle. The discovery of plate tectonics in the late 1960s showed that plates of oceanic lithosphere form at mid-ocean ridges, move away, and eventually subduct into the deep earth. It was soon recognized that seafloor depth increases approximately as the square root of lithospheric age, and that the flow of heat through the seafloor decreases similarly. Because square-root-of-time behavior characterizes diffusion processes, variations in depth and heatflow can be described by treating the lithosphere as the upper layer of a half-space that cools, thickens, and contracts as it ages. The oceanic lithosphere thus forms the cold, strong outer boundary layer of the convection system removing heat from Earth's interior.

Much old seafloor, however, is shallower than predicted by half-space cooling. This shallowing is typically treated in terms of two effects. In one, diffuse heating below most old lithosphere balances heat lost at the seafloor, causing old lithosphere to approach equilibrium thermal structure and thus depth and heatflow. However, in addition to the general "flattening" due to diffuse heating, some regional shallow swells are associated with hotspots, regions of long-lived volcanism that either are away from plate boundaries (e.g., Hawaii) or are more active than nearby portions of the plate boundary (e.g., Iceland) and have a thicker than normal crust (e.g., see Bjornsson et al., this volume). In this usage, *hotspots* refers to volcanism with no genetic implication, because it is not clear that such regions are in fact hotter than the surrounding mantle. In this paper we review the two main reference models for the thermal evolution of the lithosphere and compare the implications of each with respect to Hawaii, Réunion, Iceland, the Darwin rise, and the superswell. We begin by examining the many concepts related to hotspots and swells.

Swells are important in attempts to determine whether hotspot volcanism is due to the upwelling of plumes of hot mantle material from deep in the mantle (Morgan, 1971). In the plume model, plate motion over fixed or slow-moving plumes causes age-progressive linear volcanic chains and topographic swells that identify plumes and yield inferences about their properties. This model has been widely accepted because it gives an elegant explanation of why diverse volcanic regions have similar origins and provides an absolute reference frame describing plate motions relative to the deep mantle.

However, many hotspots deviate from the expected behavior. For instance, some hotspots move significantly relative to each other and the spin axis (Tarduno et al., 2003), changes in some volcanic chain orientations do not correspond to the expected plate motion changes (Norton, 1995), and some chains show no clear age progression (Schlanger et al., 1984; Koppers et al., 2003). Seismological results about the depth extent of the expected low-velocity anomaly differ and are being actively debated (Bijwaard and Spakman, 1999; Foulger et al., 2001; Shen et al., 2002; Montelli et al., 2004; Li et al., 2004; Dziewonski, this volume). A view is emerging that at least some hotspots, notably Yellowstone, are not due to deep mantle plumes (Humphreys et al., 2000; Christiansen et al., 2002), and the entire plume model is being both challenged (Anderson, 2000; Hamilton, 2002; Foulger and Natland, 2003; Anderson, this volume; Anderson and Natland, this volume) and defended (DePaolo and Manga, 2003; Sleep, 2003). The alternative view is that individual hotspots are due to different effects confined to the upper mantle, which might include excess melting of more fertile material (Foulger, 2002; Foulger et al., this volume), localized convective systems (King and Anderson, 1998; Humphreys et al., 2000), and cracks in the lithosphere (Jackson and Shaw, 1975; Koppers et al., 2003). Hence in discussing this issue we follow common practice in using the term *hotspot* to identify the volcanic region (which may or may not be significantly hotter than its surroundings) and *plume* for the hypothesized mantle upwelling from some unspecified source depth that causes the hotspot.

The importance of swells relative to this issue is that models for the processes causing hotspot volcanism must explain not only the volcanoes themselves but also the much broader topographic swells. For example, the Hawaiian islands cap the 200 km–wide Hawaiian topographic ridge, which is in turn flanked by the 1200 km–wide swell. The association of swells with seafloor volcanism was recognized prior to the discovery of plate tectonics. When introducing the hotspot model, Morgan (1971) noted that most hotspots were associated with shallow seafloor caused by the mantle process forming the hotspot.

In a series of papers Crough (1978, 1983) investigated this association and how it arises. Figure 1, modified from the latter paper, summarizes a set of possible models for swell formation. The first, thick sediment, was excluded because swells survive even once bathymetry is corrected for sediment loads. The second, thick crust, is insufficient because seismic refraction data show that crustal thickening occurs only within ~200 km of the volcanism (Wessel, 1993). The third, flexural uplift due to the island load, predicts a Hawaiian swell that is 600 m high at most, whereas the actual swell is ~1500 m high above the surrounding seafloor. Moreover, flexural uplift predicts a gravity anomaly smaller than observed. Hence although both crustal thickness and flexural effects contribute, they alone do not fully explain the swell (e.g., see Van Ark and Lin, 2004).

The remaining possibilities were deemed plausible and have served as the basis for many subsequent investigations. One possible cause of swell formation is compositional buoyancy arising because partial melting associated with hotspot volcanism leaves a less dense residuum after extraction of basaltic melt (Robinson, 1988). Another is the dynamic uplift that results from an upwelling plume. Finally, in the model favored by Crough (1983), a swell results from thermal buoyancy due to thermal thinning of the lithosphere by the hotspot. In this model the swell

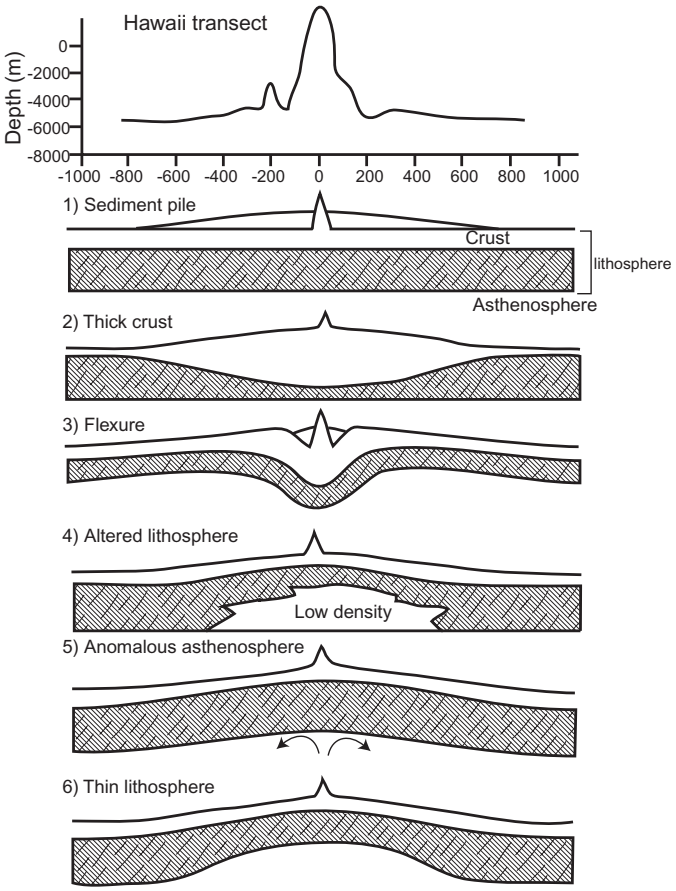

Figure 1. Top: Bathymetric profile across the Hawaiian swell. Bottom: Schematic illustrations of different processes that have been suggested to contribute to swell formation, modified from Crough, 1983. The profiles are shown perpendicular to the hotspot track; each profile represents one process that may contribute to swell formation.

would also have higher-than-normal heatflow, and both the heatflow and uplift would decrease as the plate moved away from the hotspot.

Twenty years later, the basic framework for discussions of swells has changed little. Each of the competing hypotheses—and combinations thereof—have been explored extensively in the literature. However, as this volume illustrates, no consensus has emerged about the existence of mantle plumes, how hotspots arise, and how these processes cause the associated swells.

Various lines of evidence have been used to constrain, test, and argue for and against the different models. Successful models should predict the many ways in which swells differ from oceanic lithosphere of similar age elsewhere, including ocean depths, seafloor heatflow, gravity, crustal thickness, and seismic velocity structure. We focus here on two of these, depth and heatflow. Hence we ask, How much of a swell exists at hotspot swells, and how hot—in the sense of surface heatflow—are they? It turns out that these simple questions are surprisingly difficult and admit a range of answers. Of these, the most plausible exclude significant heatflow anomalies and hence substantial thermal thinning of the lithosphere.

REFERENCE MODELS

Assessing the depth and heatflow anomaly due to a hotspot involves comparing the depth and heatflow to a reference model predicting depth and heatflow for "normal" oceanic lithosphere as functions of age (Fig. 2). The primary surface observables constraining these models are variations in seafloor depth and heatflow with lithospheric age (Table 1). In the models, seafloor depth depends on temperature integrated through the lithosphere, whereas heatflow depends on the temperature gradient at the seafloor.

The simplest such model is one in which the lithosphere evolves as the upper boundary layer of a cooling half-space as it moves away from mid-ocean ridges (Davis and Lister, 1974). This model describes the observation that depth and heatflow vary approximately with the square root of lithospheric age.

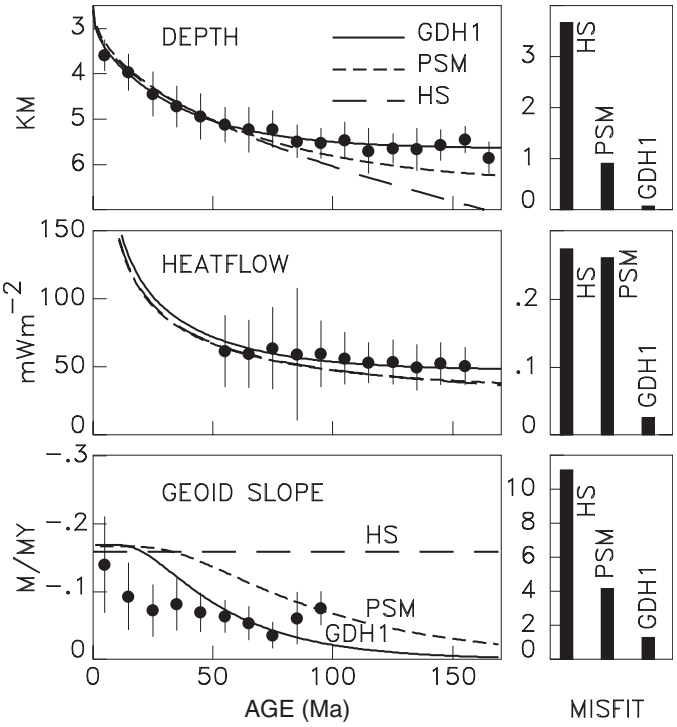

Figure 2. Comparison of the predictions of the three thermal models to data not used in deriving the models. Global depth data exclude hotspot swells (Kido and Seno, 1994). Global heatflow data are from Stein and Stein, 1992, which used only north Pacific and northwest Atlantic values to derive model GDH1. The geoid slopes across fracture zones are from Richardson et al. 1995. The misfit values (right panels) show that the GDH1 thin-plate model fits better than either a half-space (HS) model or the thick-lithosphere model of Parsons and Sclater (1977) (PSM). From Richardson et al., 1995.

TABLE 1. CONSTRAINTS ON THERMAL MODELS FOR TEMPERATURE AS A FUNCTION OF DEPTH AND AGE $T(z,t)$

Observable	Proportional to	Reflects
Young ocean depth	$\int T(z,t)dz$	αT_m
Old ocean depth	$\int T(z,t)dz$	$\alpha T_m a$
Old ocean heatflow	$\frac{\partial T(z,t)}{\partial z}\,\mathrm{i}_{z=0}$	T_m/a
Geoid slope	$\frac{\partial}{\partial t}\int zT(z,t)dz$	$\alpha T_m\, exp(-t/a^2)$

Notes: a—plate thickness; T_m—basal temperature; α—coefficient of thermal expansion. The half-space model corresponds to $a \rightarrow \infty$.

However, for ages older than ca. 70 Ma, depth and heatflow "flatten," varying more slowly with age than for a half-space. It is thus generally assumed that half-space cooling is perturbed by additional heat from below, which balances the heat lost at the seafloor, stops the lithosphere from continuing to cool for older ages, and thus causes flattening. The plate model, a simple and common description of this perturbation, uses an isothermal boundary at the base of the lithosphere to model the thermal equilibration of old lithosphere (Langseth et al., 1966; McKenzie; 1967). The plate model fits the data reasonably well, but does not directly describe how the heat is added from below (Crough, 1977; Parsons and McKenzie, 1978; Doin and Fleitout, 1996). Although the predictions of the plate and half-space models are the same for young ages, the results are different for ages great enough that the basal condition has an effect.

The first commonly used plate model, based on parameters estimated by Parsons and Sclater (1977; denoted PSM) was subsequently found to systematically overpredict depths and to underpredict heatflow for most old lithosphere, implying widespread depth and heatflow anomalies. Thus regions were considered anomalous even though they did not differ from others of similar age.

This situation prompted a joint inversion of depth and heatflow data, which found that these anomalies were reduced significantly by a reference model termed GDH1 (Stein and Stein, 1992). GDH1 is characterized by a plate with an asymptotic thermal thickness of 95 ± 10 km, thinner than the previously estimated 125 ± 10 km–thick plate, and a basal temperature of 1450 ± 100 °C, consistent with the previous estimate of 1350 ± 275 °C. As a result, the lithosphere is hotter at depth and so has higher heatflow and less subsidence. This model also better fits depth, heatflow, and satellite gravity data not inverted in deriving GDH1(Stein and Stein, 1993). The better fit of GDH1, or similar thin-plate models, is robust. It occurs even for depth datasets from which swells are excluded (Shoberg et al., 1993; Kido and Seno, 1994). Satellite geoid data are also diagnostic, because geoid slope, the gradient of the geoid in the direction of increasing lithospheric age, should be constant with age for a half-space model, but in plate models "rolls off " at older ages at a rate depending inversely on plate thickness (Cazenave, 1984; Table 1). A thin-plate model better fits geoid slope observed both across fracture zones (Richardson et al., 1995) and oceanwide (DeLaughter et al., 1999).

Figure 3 illustrates how the choice of reference model influences what we perceive as "anomalous" in the broad region of the Pacific containing the Hawaii hotspot track. Relative to a half-space, almost the entire region is anomalously shallow. Relative to the PSM plate model, the swell is quite broad, whereas relative to GDH1, the swell is narrower. Similarly, although this and other swells have high heatflow relative to PSM, these heatflow anomalies are reduced dramatically using a thin-plate model (Stein and Stein, 1993). As a result, the thermal reheating models for swells no longer seem viable.

This example illustrates the generalization that what we regard as "anomalous" depends on what we define as "normal." This choice implicitly reflects both our biases about the underlying physics and the data we select. For example, plate models assume that there is a "typical" state of old lithosphere with shallower depths and higher heatflow than for a half-space, from which hotspot swells reflect deviations. In contrast, Crough (1978, 1983) assumes that half-space cooling is "typical," but that so much of the ocean basins have been affected by hotspot swells that the general flattening at old ages is due to their cumulative effect. Which of these views one adopts is a matter of philosophical choice and dictates one's view of swells.

GDH2 MODEL

The recent revival of interest in hotspots and the mechanisms causing them prompted us to revisit the issues of reference models and the resulting anomalies. Our approach, illustrated schematically in Figure 4, follows the familiar process used to derive reference models that describe a large set of data in terms of a simple physical model characterized by a relatively small, or sparse, set of parameters. The models are used to characterize large sets of data in a simple way and thus identify misfits or "anomalies" in which data deviate from the model predictions. We then use reference models to draw inferences about the processes that give rise to both the average situation and deviations from it. For example, models of average global seismic velocities are used to constrain models of the average radial variations in composition and temperature and as a reference against which velocity perturbations due to subducting slabs, continental roots, hotspots, ridges, and so on can be identified and analyzed in terms of local processes that perturb the global model. Similarly, plate motion models using Euler vectors are a simple description of rigid plate behavior, and places where geodetic data or earthquake mechanisms deviate from these predictions indicate deviations from rigid plates.

As illustrated in Figure 4, the models are refined over time. In each cycle, new model parameters are estimated by reducing

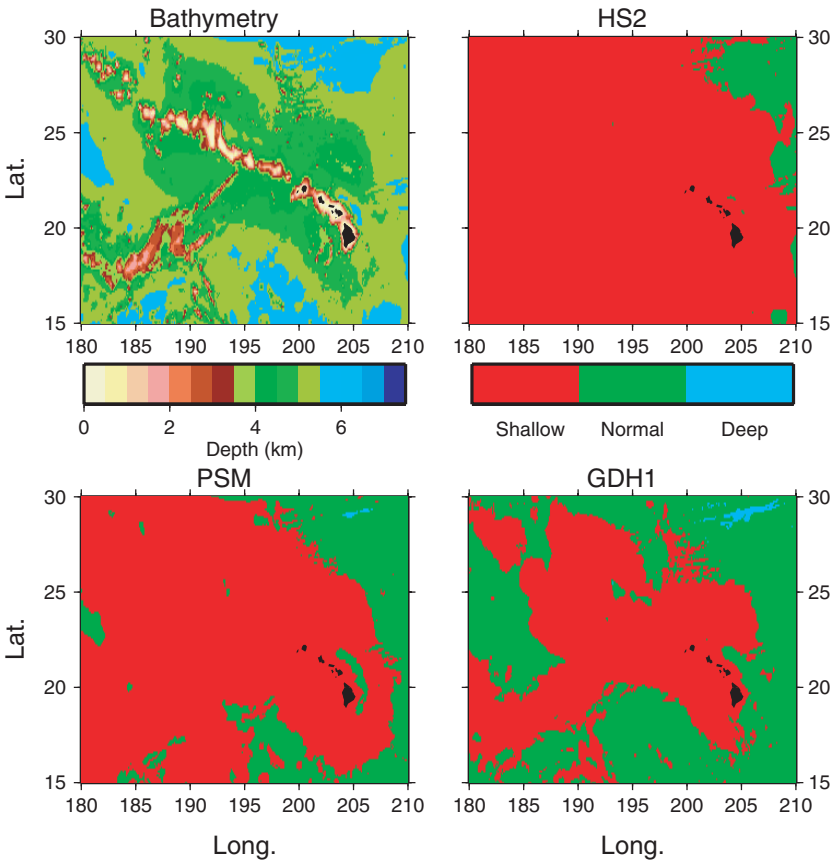

Figure 3. Upper left: Seafloor topography near Hawaii, corrected for sediment loading. Other panels: Depth anomaly maps for different reference models. The anomalies are divided into those within 500 m (about one data standard deviation) of that predicted (green), those shallower (red), and those deeper (blue). Relative to a half-space (HS) model or the model of Parsons and Sclater (1977) (PSM), most of the area is anomalously shallow, as would be the case for most lithosphere of this age. However, relative to GDH1 the swell is narrower.

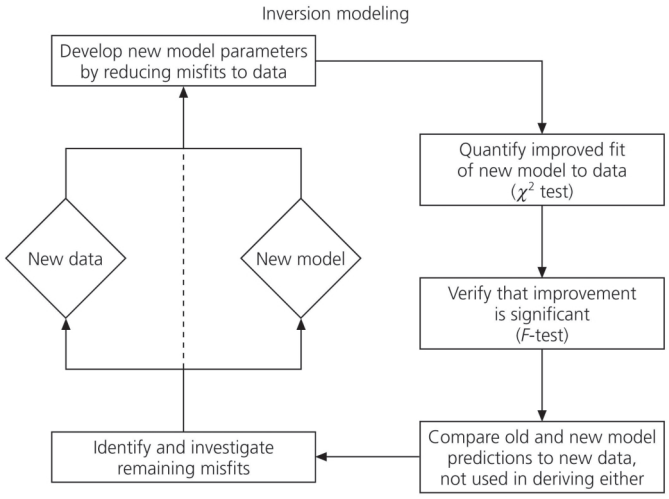

Figure 4. Schematic illustration of how models are refined over time using new data and model parameterizations, and then tested.

the misfits to data. The remaining misfits are treated as "anomalies" and investigated. At a later stage, the cycle is repeated using new data, new model parameterizations, or both. Eventually the reference model does not improve significantly. When this occurs, we are likely doing about as well as is possible with this type of model. For example, laterally homogeneous global seismic velocity models have become sufficiently accurate that more attention is now directed toward the lateral variations. Similarly, even the best possible global reference model for depths as a function of age cannot describe the range of depths that occur for lithosphere of a given age. This is because the simple model assumes that the only process is cooling of a plate with uniform physical properties, whereas the real Earth has varying properties, and depths and heatflow also depend on effects other than plate cooling. For example, the model does not include the effects of hydrothermal circulation, which reduces the measured heatflow in lithosphere younger than 50 Ma lower than that predicted. It similarly does not incorporate crustal thickness variations, which can perturb depths.

It is worth bearing in mind that the resulting reference model, like the solutions to other inverse problems, is not unique, exact, or "correct." Because the data are scattered and the models simplify complex reality, no model exactly describes the data. Similarly, a range of parameters can describe the data equally well for a given model, we can select the data in various ways, and we have various models to choose from based on various criteria and preconceptions. For example, we can invert either the entire global depth dataset or one that excludes swell regions that have been defined based on some a priori criterion. The resulting models depend on these choices. For example, Parsons

and Sclater (1977) inverted the deepest depths in a given age range in the north Atlantic and the north Pacific, whereas Stein and Stein (1992) inverted mean depths. Similarly, Parsons and Sclater (1977) reduced the measured heatflow to correct for then-expected radioactive heat production, which now seems too high, whereas Stein and Stein (1992) did not. As a result, the GDH1 inversion yielded a model with a hotter and thinner lithosphere, and hence predicted shallower depths and higher heatflow for old lithosphere.

Another point worth recognizing is that most thermal models for the lithosphere are phenomenological in that each is derived to be the simplest model that describes the observed variation in depth and heatflow. These variations may in part also reflect other possible effects, some of potential significance, which are not included in the model. Of special importance for our discussion here is that the variation in depth with age is assumed to result entirely from the temperature structure of the lithosphere (Parsons and McKenzie, 1978), whereas depth effects can also reflect sublithospheric processes (Hager and O'Connell, 1980; Buck and Parmentier, 1986; Davies, 1988; Jarvis and Peltier, 1989). In addition, the plate model used here does not incorporate time-dependent effects beyond cooling, such as might be associated with the proposed Cretaceous superplume (Larson, 1991). Determination of the magnitude of these possible effects not included in the plate model has long been challenging precisely because the simple plate model fits the two primary surface observables, depth and heatflow, reasonably well. Although the depth-age and heatflow-age curves are derived assuming a thermal model, their utility is not directly tied to the appropriateness of the thermal model, and we do not ascribe great significance to the details of the predicted temperature structure, especially in the lower lithosphere. Similarly, in comparing models it is useful to compare their predictions rather than the nominal parameters. Models that are nominally different when quoted in terms of plate thickness, basal temperature, coefficient of thermal expansion, and so on can be quite similar in their predictions for the observables in Table 1 (Stein and Stein, 1993). As a result, we think of models in broad classes, e.g., thin versus thick lithosphere.

Many of these issues have long been recognized in the broader context of the role of models in science. Models are held to reflect the processes and characteristics of the system being studied but are useful only insofar as they provide a simple and reliable description of the observations and predictions (Popper, 1935). Thus a model that describes the majority of observations with few exceptions is held to be better than one that has more outliers for the same set of observations. As new observations are added, or old datasets are refined, the best model can change in a manner analogous to Hegel's (1816) "thesis, antithesis, synthesis." In every model, some data points will inevitably remain outliers; this may be due to errors in measurement or poorly selected parameters, or the data points may be indicators of other processes. The advantage of a better-fitting model is that it reduces the number of outliers that must be investigated. It avoids a situation in which most of the data are considered anomalous, as in the "Lake Wobegon effect" (Stein and Stein, 1997), named for the fictitious town wherein "all children are above average."

Our analysis here follows the general approach and inversion method of Stein and Stein (1992). However, we use newer data on global bathymetry (Smith and Sandwell, 1997), age (Mueller et al., 1997), and sediment thickness (http://www.ngdc.noaa.gov/mgg/sedthick/sedthick.html; from D. Divins, 2004) and include data on geoid slope (Nerem et al., 1994). In addition, we use a spatial filtering technique based on the ratio of geoid to topography to exclude areas such as swells that deviate from age-dependent behavior. Like DeLaughter et al. (1999), we use the absolute value of the gradient of the geoid to topography ratio (GTR) and exclude values greater than 5 mm/km^2. In this application, we use the ETOPO5 topography dataset rather than newer data because the latter derive the topography from the geoid, so its use might introduce some bias. This window function eliminates a variety of presumably anomalous topographical features, including many of the swells, as illustrated (Fig. 5) by comparison with a hotspot map developed by Sleep (1990) using swell heights. The data were placed in 5 m.y. bins and inverted to derive a model termed GDH2 by DeLaughter et al. (1999).

Here we explore the robustness of this approach by deriving several variants on the model. In GDH2A we inverted the global dataset and left the basal temperature as a free parameter, as we did for GDH1, rather than fixing it as in GDH2. GDH2B used GTR-restricted data and inverted for all parameters. The GDH2C inversion was run using all data and a 2600 m ridge crest depth. GDH2A and GDH2B used a 2810 m ridge crest depth, based on sample transects. The deeper ridge crest depth was derived by fitting a simple linear trend for ages younger than 20 Ma to bathymetry profiles from the Atlantic and Pacific ridges.

The resulting model parameters are listed in Table 2. The models derived from them are similar to GDH2, and hence provide similar fits to the data (Fig. 6). The predicted depths are somewhat shallower than the predictions of GDH1, presumably because GDH1 (and PSM) were derived using data from the north Atlantic and the north Pacific, whereas the Indian Ocean is shallower (Shoberg et al., 1993). The depth and heatflow predictions for GDH2 may be conveniently and accurately approximated using a half-space model with the same parameters for young lithosphere and the first term of the series solution, with $R >> \pi$ for older lithosphere (Parsons and Sclater, 1977). The depth (d), in meters, is related to the age (t), in Ma, by

$$\begin{aligned} d(t) &= 2600 + 349t^{1/2},\ t < 16 \text{ Ma} \\ &= d_r + d_s\,[1 - (8/\pi^2)\exp(-\kappa\pi^2 t/a^2)] \\ &= 5302 - 2190\exp(-0.0323t),\ t \geq 16 \text{ Ma}, \end{aligned}$$

where κ is thermal conductivity, and the heatflow (mWm^{-2}) is **Correct?**

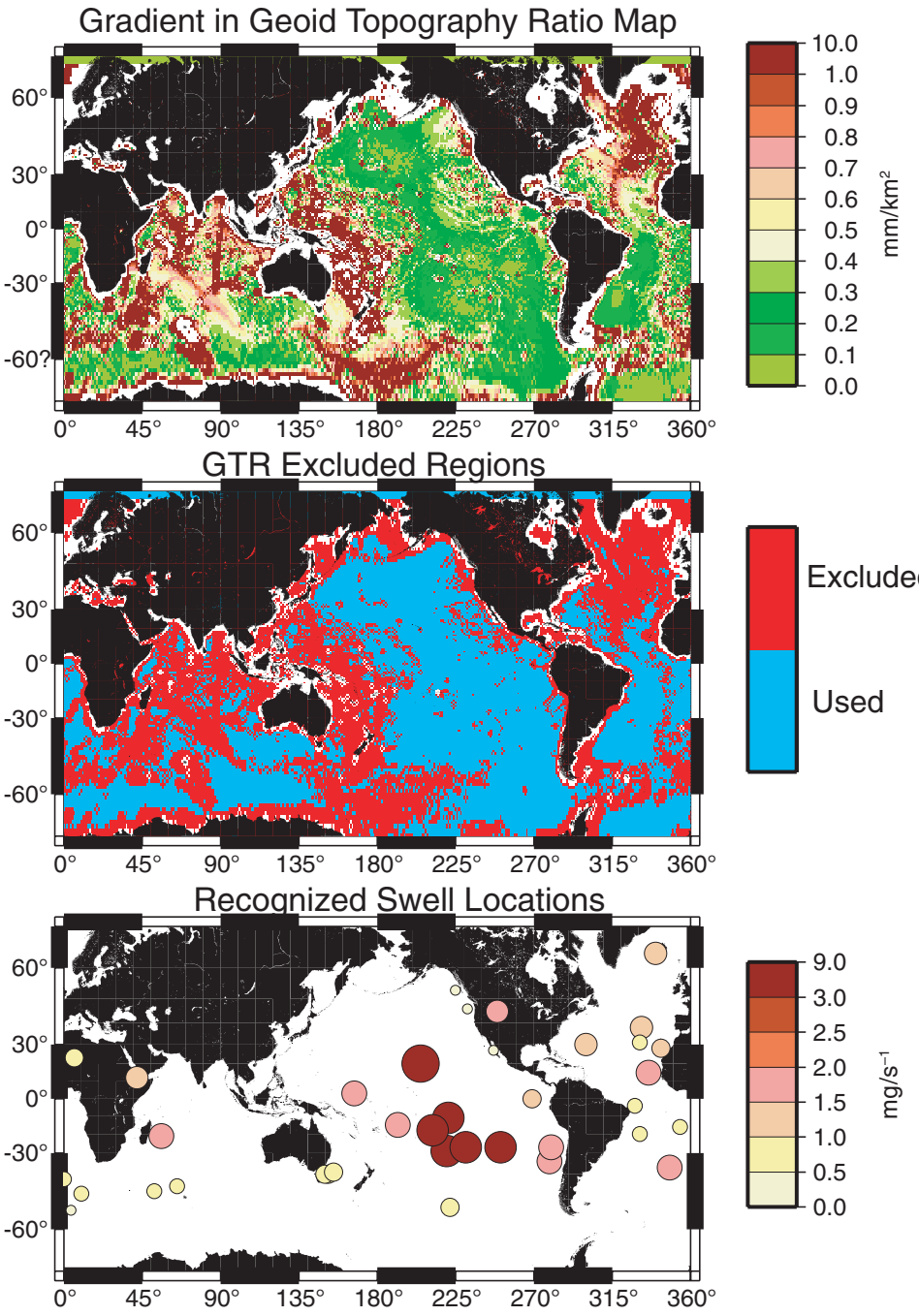

Figure 5. Top: The gradient of the geoid to topography ratio (GTR) is shown in units of mm/km^2. Center: Global depth data excluded by the gradient GTR filter (shown in red) for values greater than the absolute value of 5 mm/km^2. The depth, geoid slope, and heatflow data used to derive GDH2 are from regions with gradients of GTR between –5 and 5 mm/km^2 (blue areas). Bottom: Hotspot map, with the colors and sizes of the circles based on flux (units in Mg/s^{-1}) inferred from swells by Sleep (1990). The largest circles are for fluxes ≥3.0 Mg/s^{-1}, and the smallest are for fluxes ≤1.0 Mg/s^{-1}.

$$q(t) = 481\ t^{-1/2},\ t < 44 \text{ Ma}$$
$$= q_s\ [1 + 2\ exp\ (-\kappa\pi^2 t/a^2)]$$
$$= 48.8 + 97.5\ exp\ (-0.0323t),\ t \geq 44 \text{ Ma},$$

Please fill in definition.

where q is _____.

Figures 7 and 8 show the depth and heatflow anomalies for the half-space, PSM, and GDH2 models. Some depth anomalies occur only relative to a half-space, whereas others remain for the other models but have smaller widths and amplitudes. For example, as in Figure 3, the swells are much narrower for GDH2. Interestingly, although the GDH2 heatflow anomalies are roughly equal (i.e., as many regions are too cold as are too hot), the depth anomalies are not (though they are more evenly distributed than for the other models). This is probably a side effect of the inversion methodology; because all three datasets were given equal weighting, the set with the largest error dominated the inversion.

TABLE 2. INVERSION RESULTS

Model	α	k	H	T_m	Ridge depth	χ^2
HS2	3.50	2.50	n.a.	1350	2600	3.503
PSM	3.28	3.14	125	1350	2500	2.662
GDH1	3.10	*3.14*	95	1450	2600	1.996
GDH1A	3.25	3.65	100	*1350*	2600	2.252
GDH2	3.10	3.25	90	*1350*	2600	1.506
GDH2A	3.65	3.10	85	1350	2810	2.568
GDH2B	3.25	3.00	90	1400	2810	1.992
GDH2C	3.25	2.90	90	1450	2600	1.841

Notes: α in $10^{-5}K^{-1}$, k in W m^{-1} K^{-1}, H in km, T_m in °C, ridge depth in m. Italics indicate fixed parameters. GDH1 inversions were for depth and heatflow only; HS2 and GDH2 inversions were for depth, heatflow, and geoid slope. GDH2 and GDH2B used GTR-restricted data. GDH2A and GDH2C used all data. GDH2A and GDH2B used a deeper ridge crest, based on sample transects. χ^2 values were found by comparing global datasets in increments of 1 m.y. to model predictions and were computed in a manner similar to that used by Stein and Stein (1992). For GDH2, mantle density was fixed at 3300 kg/m^3, water density was fixed at 1000 kg/m^3, and the specific heat was fixed at 1171.5 J kg^{-1} K^{-1}.

These figures bear out the complexity of processes that may be operating beyond simple lithospheric cooling. For example, a broad, shallow anomaly in the north Atlantic extends well south of Iceland (e.g., see King, this volume). Similarly, GDH2 reduces the extent of shallow depth and high heatflow anomalies in old lithospheric areas such as Hawaii, but heatflow in young lithospheric areas near spreading ridges is still lower, and ridge depths deeper, due to hydrothermal circulation (e.g., Cochran and Buck, 2001). Alternatively, DeLaughter (1998) and Hofmeister and Criss (this volume) have suggested that the mantle conditions underlying the lithosphere may be neither isothermal nor homogenous.

HAWAII AND OTHER MIDPLATE SWELLS

We have used the GDH models to examine possible anomalies at a variety of hotspot swells on old (older than 50 Ma) lithosphere, where we expect that the model should provide a good characterization of unperturbed lithosphere. Such midplate swells are exemplified by the Hawaiian swell, the largest and best studied. Hawaii is the type example because of its size and its isolation from other perturbing processes, including ridges and other hotspots.

Interpreting the heatflow data for Hawaii shows many of the issues associated with using reference models. The observation that heatflow measurements made parallel to the axis of the Hawaiian swell (Fig. 9A) were higher than that predicted for a halfspace model with PSM parameters was initially treated as consistent with the elevated heatflow expected for a reheating model, which matched the depth anomalies, where the bottom of the lithosphere is reheated to asthenospheric temperatures to a 40–50 km depth (Fig. 9B; Von Herzen et al., 1982). However, a subsequent transect perpendicular to the swell axis at the site of the predicted maximum anomaly (Fig. 9C) showed that the heatflow did not vary with the expected pattern; rather it at most slightly differed compared to lithosphere of comparable ages elsewhere (Von Herzen et al., 1989). Thus much of the apparent anomaly resulted from comparing the heatflow to cooler reference models, which systematically underpredict the heatflow for old lithosphere, so the measurements did not support substantial lithospheric reheating.

Data for the Hawaiian swell region (Fig. 10A, top), including denser recent sampling by Harris et al. (2000a), show no pattern of a significant increase in heatflow (Fig. 10A, bottom) or heatflow anomaly (Fig. 10B, top) northwest of Hawaii. The heatflow anomaly is essentially constant from 800 km, before volcanism starts at Hawaii, to over 800 km northwest of Hawaii, ~5 mWm^{-2} above the GDH2 global predictions. (Though some data exist for sites farther to the southeast beyond the region discussed, generally those sites are even sparser and the values more scattered, so they were not included here.) The area surrounding Maro Reef, affected by the hotspot ca. 20 Ma, is at most about a few mWm^{-2} higher heatflow compared to the southeastern portion of the track.

However, the amount of reheating predicted depends on the model (temperature increase, depth of reheating, timing of reheating, width of reheating perpendicular to the swell axis, etc.) and the choice of a zero reference. For example, the observed pattern of the heatflow anomaly may be compared to a simple model of a 100 km sill emplaced into the lithosphere with a temperature difference of 250 °C (Von Herzen et al., 1989; Bonneville et al., 1997). A wide range of asthenospheric temperatures associated with Hawaii and perhaps other hotspots have been suggested, up to ~250 °C higher than normal. For further discussion see Clague et al., 1995; Green and Falloon, this volume; Presnall and Gudfinnsson, this volume.

The predicted heatflow anomaly is shown in Figure 10B for 10 km increments in reheating depth from the shallowest reheating depth of 40 km to 90 km. If GDH2 is chosen as the baseline(Fig. 10B, top), the heatflow data may be used to infer reheating to 40–50 km. Given that GDH2 is a global average and that regional depth differences occur, it is natural to assume that regional differences in heatflow occur. Hence, if the baseline is the average of the heatflow measurements on the incoming lithosphere and thus somewhat higher than GDH2, no heatflow anomaly is observed within the Hawaiian islands, and the data at Maro Reef suggest at most 60 km, if not deeper reheating depths (Fig. 10B, bottom). If thermal thinning does not reach its maximum until Kauai, as suggested in a recent seismic study (Li et al., 2004), the maximum heatflow anomaly would be ~500 km farther to the northwest of Maro Reef. However, because the predicted heatflow change between 15 and 20 Ma is relatively small (Fig. 9B and Fig. 10B), the estimation of reheating depths is about the same.

Some (e.g., Harris et al., 2000b; McNutt, 2002) have suggested that hydrothermal circulation may mask the thermal

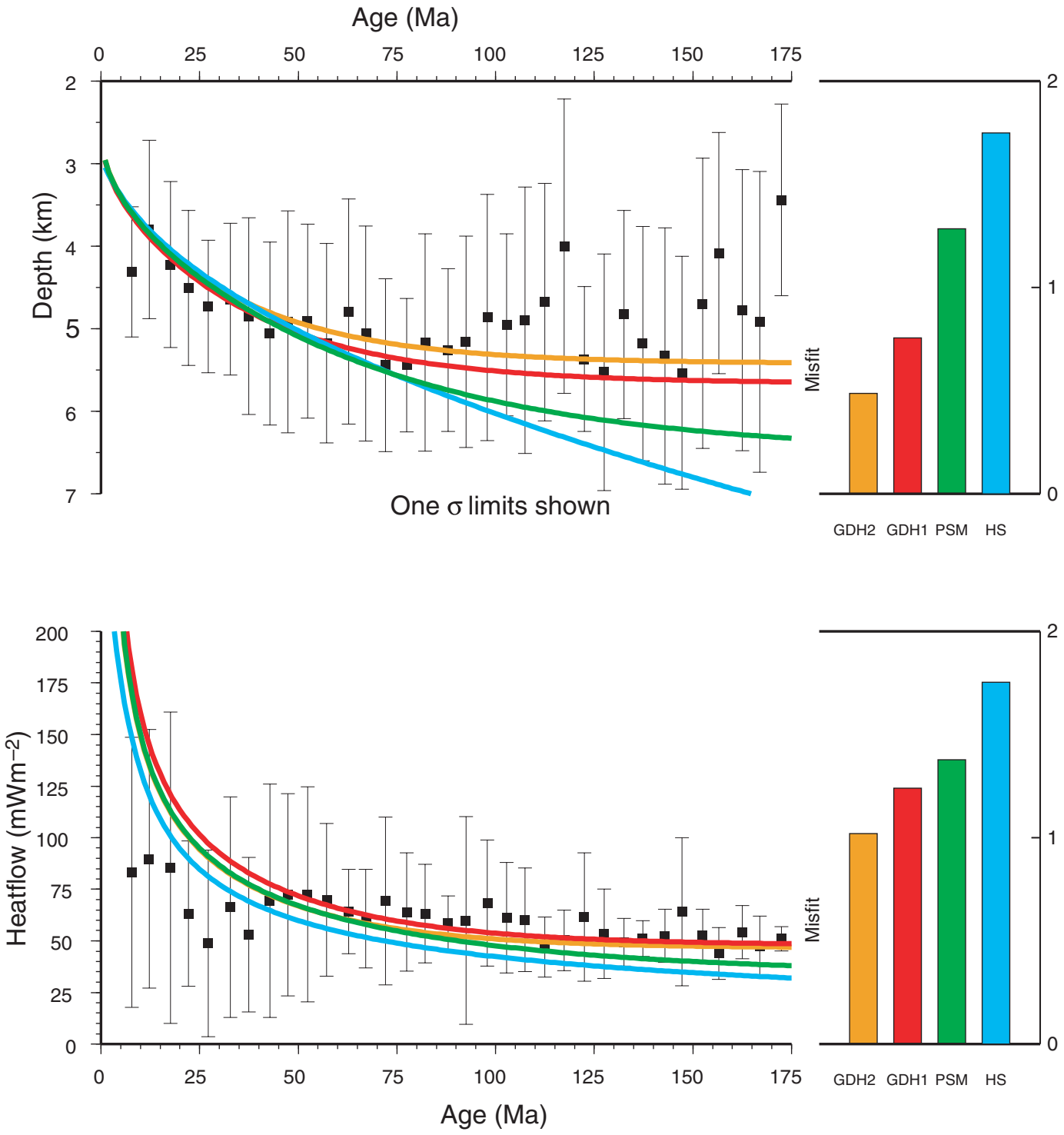

Figure 6. Comparison of fits for the half-space, PSM, GDH1, and GDH2 models to the global depth and heatflow data in 5 m.y. bins. Misfits are calculated in a manner similar to that used by Stein and Stein (1992). PSM—Parsons and Sclater (1977) model.

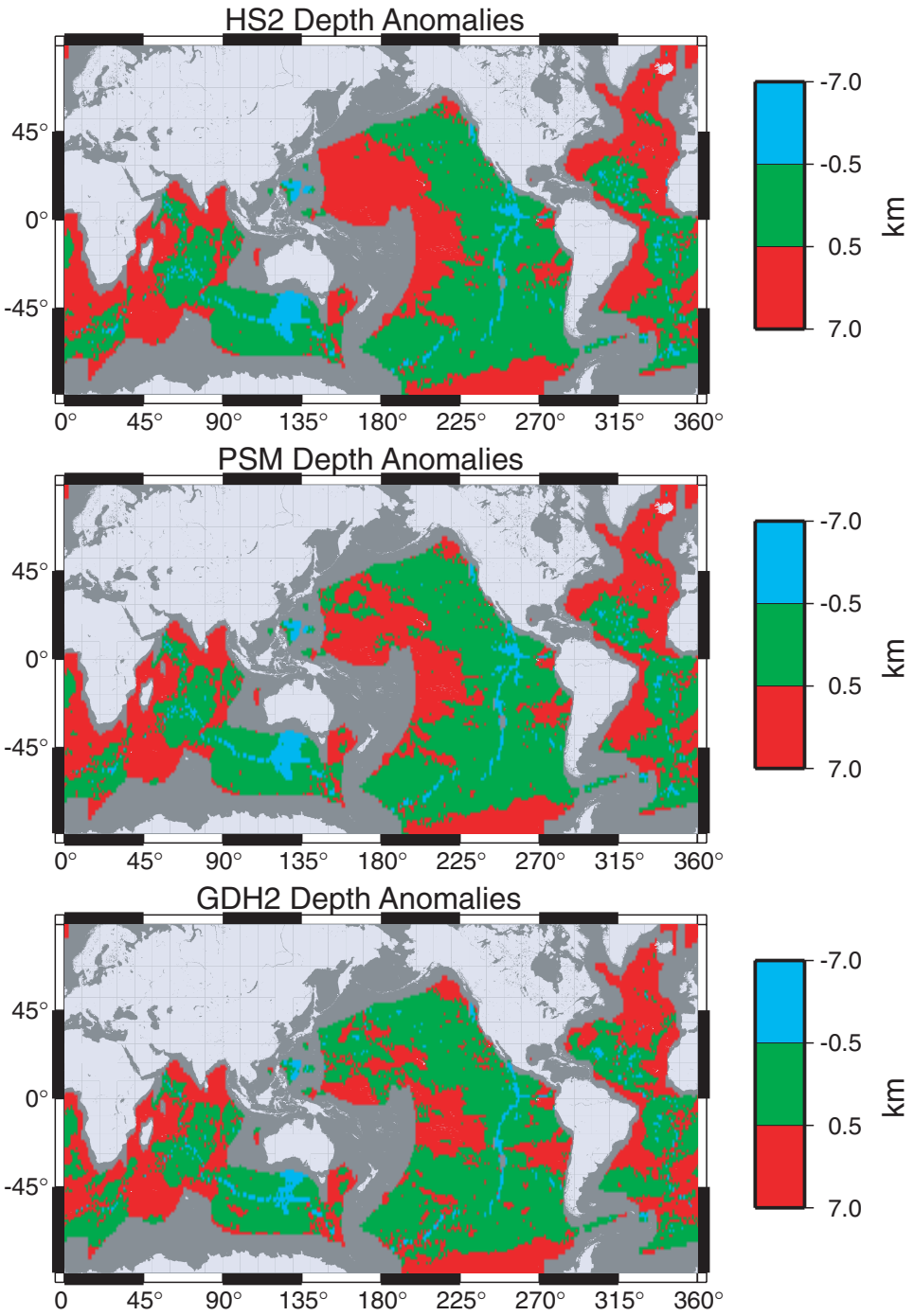

Figure 7. Depth anomalies for the half-space, PSM, and GDH2 models. Depth bins in kilometers. PSM—Parsons and Sclater (1977).

signature of major lithospheric reheating in a manner analogous to the widely recognized patterns at ridge crests or smaller seamounts. However, while calculations (Harris et al., 2000b) suggest that there may be removal of heat by hydrothermal circulation within ~150 km of the axis of the Hawaiian islands (over the deeper parts of the moat), it does not explain the absence of a heatflow anomaly farther away. Nor do the calculations for hydrothermal circulation explain why measured heatflow (Harris et al., 2000a) is higher at Oahu (affected by the hotspot ca. 4 Ma) compared to the somewhat lower heatflow at Maro Reef (affected by the hotspot ca. 20 Ma). The Oahu heatflow sites are near the North Arch volcanic field (J. Natland, 2004, personal commun.), but it is uncertain what, if any, thermal effect results here because the age, lateral extent, and thickness of the volcanic field are not well known. We therefore conclude that hydrothermal circulation is unlikely to mask regional heat-

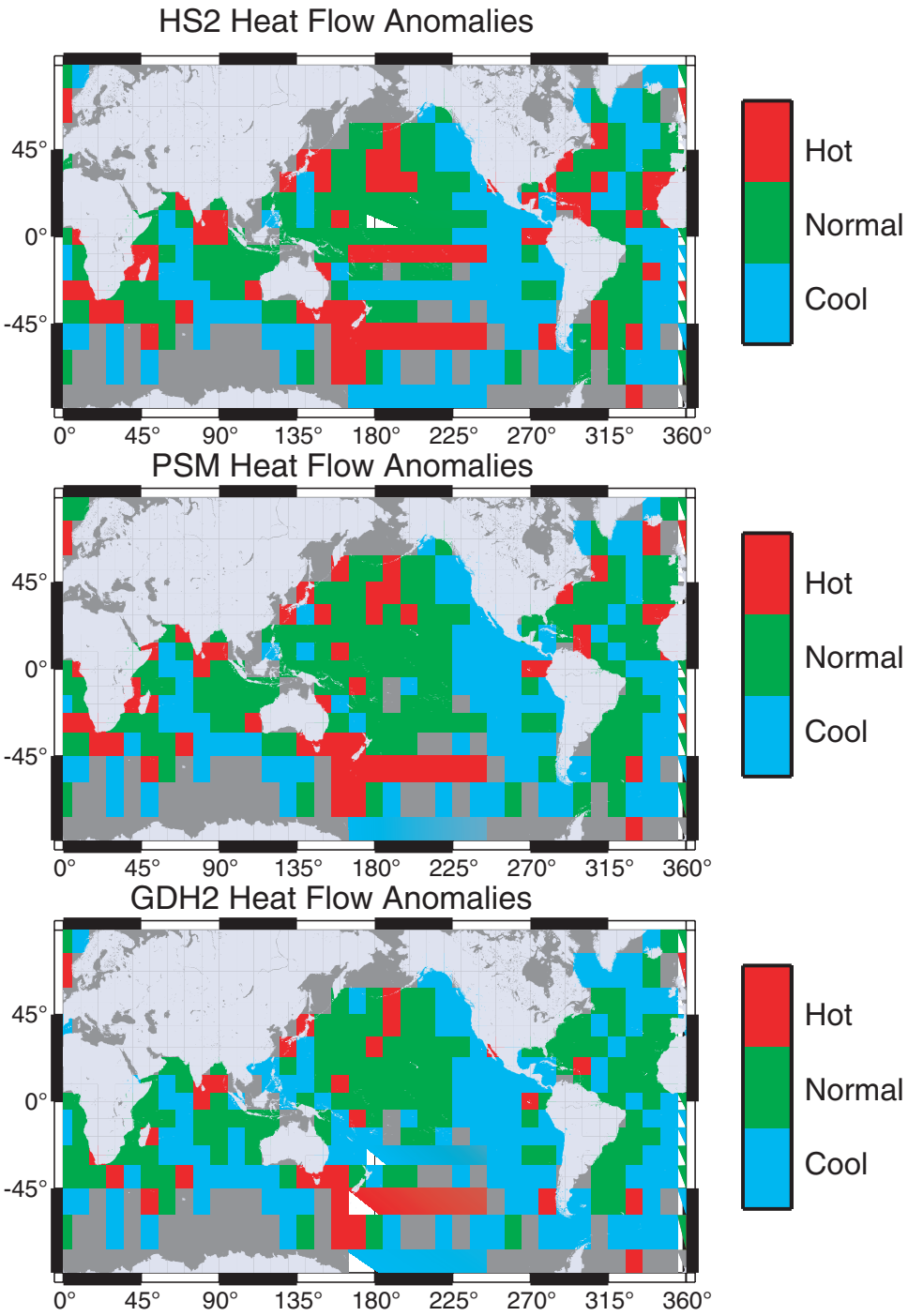

Figure 8. Heatflow anomalies for the half-space, PSM, and GDH2 models (PSM—Parsons and Sclater, 1977, model). The anomalies are divided into those within 15 mWm^{-2} of that predicted (green), those larger (red), and those smaller (blue). The anomalies are shown for 10° by 10° regions with a minimum of three measurements.

flow anomalies due to significant lithospheric reheating (e.g., see Von Herzen et al., 1982).

The lack of temporal (or spatial) heatflow variation parallel and perpendicular to the swell (Von Herzen et al., 1989; Harris et al., 2000a) seems to exclude shallow reheating and favor either deep reheating, which would not yet significantly perturb the surface heatflow, or the dynamic effects of a mantle plume, which would have similar effects (Liu and Chase, 1989). The associated compositional buoyancy (Sleep, 1994) could also contribute to the uplift but could not alone be responsible for the later subsidence. It is worth noting that most seismological studies show no evidence for a low-velocity zone under the swell (e.g., Woods et al., 1991).

A similar situation applies for other hotspot swells, where heatflow data show a large anomaly with respect to a thick-plate or half-space model, but a smaller one with respect to a thin-

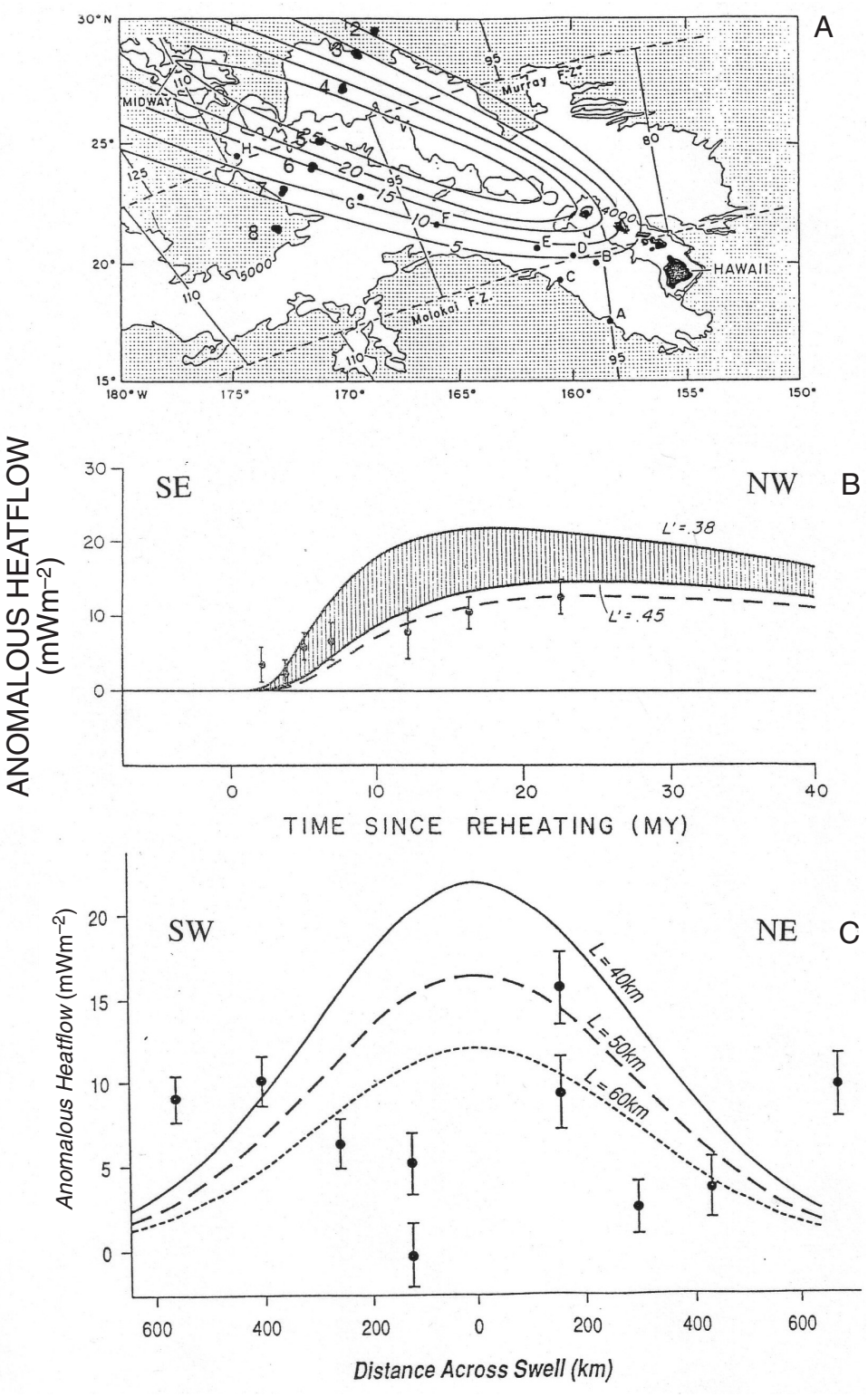

Figure 9. (A) Illustration of the hotspot reheating model, showing the expected temporal variations in depth and heatflow for the Hawaiian swell. This model assumes instantaneous lithospheric reheating to asthenospheric temperatures over a 300 km–wide region perpendicular to the swell axis. (B) The heatflow data (for sites A–H) shown, given as anomalies with respect to the half-space model using the parameters of the Parsons and Sclater (1977) model (PSM), were initially interpreted as evidence for reheating at a depth of ~40–50 km (Von Herzen et al., 1982). L′ represents the nondimensional lithospheric thickness after initial reheating. (C) The heatflow data (for sites 1–8), given as anomalies with respect to 50 mWm^{-2}, the observed approximate average for old crustal sites, do not show the variation expected for shallow lithospheric reheating (Von Herzen et al., 1989). The two different heatflow values at ±150 km are two different corrections for sediment blanketing effects for the same sites. L indicates the lithospheric thickness after the initial thermal thinning.

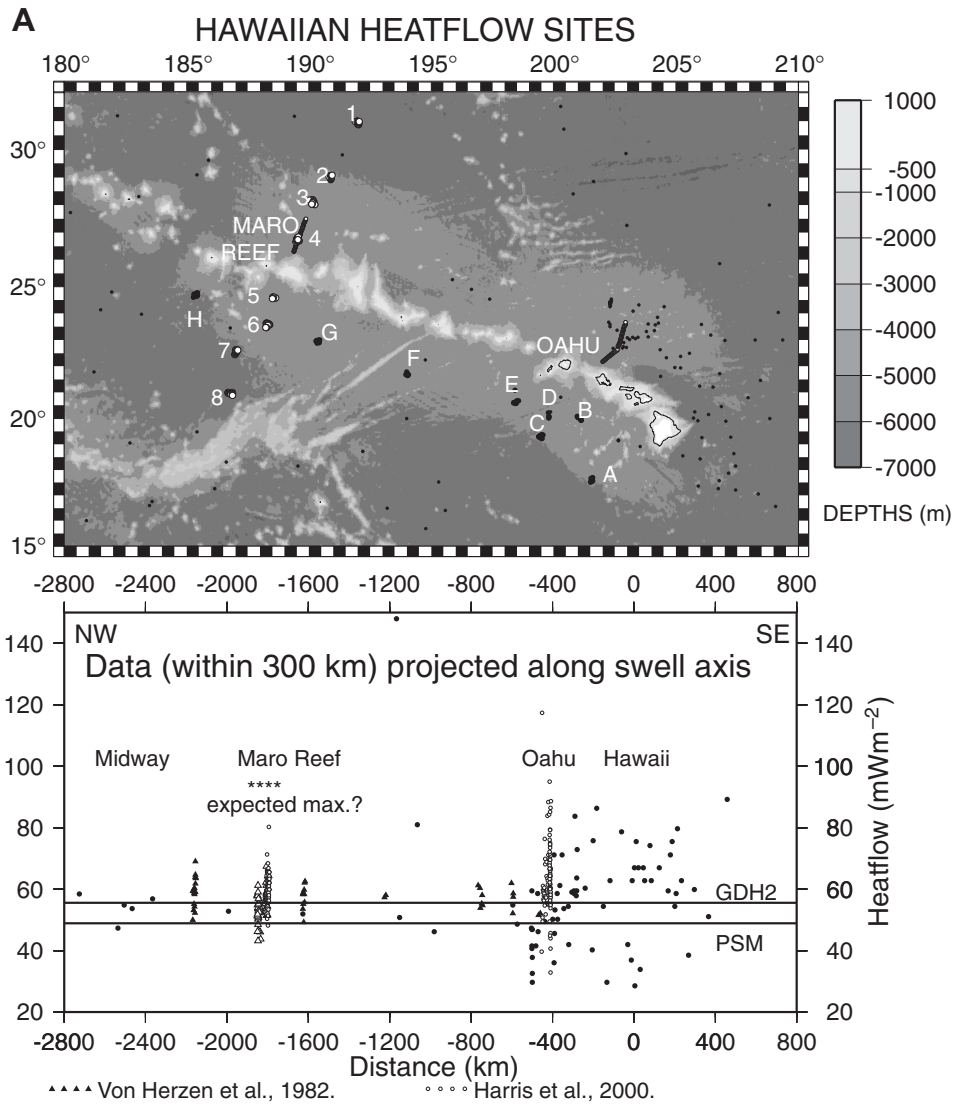

Figure 10. (A) Top: Heatflow data recorded near Hawaii. Bottom: Heatflow data projected along the axis of the Hawaiian swell. The possible anomaly is smaller with respect to GDH2 than the model of Parsons and Sclater (1977) (PSM) and does not show the expected variation along the swell (Fig. 9). (B) The heatflow anomaly relative to GDH2 (top) and relative to the average incoming heatflow southeast of Hawaii (bottom). The inferred depth of reheating (orange lines) depends on the choice of the reference.

(continued)

plate model. Figure 11 shows this effect for the Réunion hotspot, and the Bermuda, Cape Verde, and Crozet swells behave similarly (Stein and Stein, 1993).

YOUNG LITHOSPHERE

The Superwell

For younger lithosphere the thermal models systematically overpredict the observed heatflow (Fig. 6), because they assume that all heatflow occurs by conduction, whereas hydrothermal activity appears to transport a significant fraction of the heat (e.g., Stein and Stein, 1994). Hence in these areas we compare the swell heatflow to the observed global average for lithosphere of that age. As shown in Figure 12, the mean heatflow varies smoothly with age, although there is scatter due to high and low values associated with up- and down-going water flow (Stein, 2003).

This approach is useful for studying the superswell, an area from west of the East Pacific rise to ~160°W, 9–30°S that is substantially shallower than expected for its 20–90 Ma age (Fig. 13). Menard (1984) believed this area, termed the Polynesian Plume Province by Vogt (1981), contained both a broad regional uplift and a number of hotspot swells, including the Cook-Austral, Marquesas, Pitcairn, and Society seamount chains. These hotspot tracks have formed volcanic edifices in the past 18 m.y. (Duncan and Clague, 1985), giving rise to a complex pattern of volcanic ages and types. Holocene volcanism occurs at several sites on the chains, and the NW-SE trend of the plateaus and island

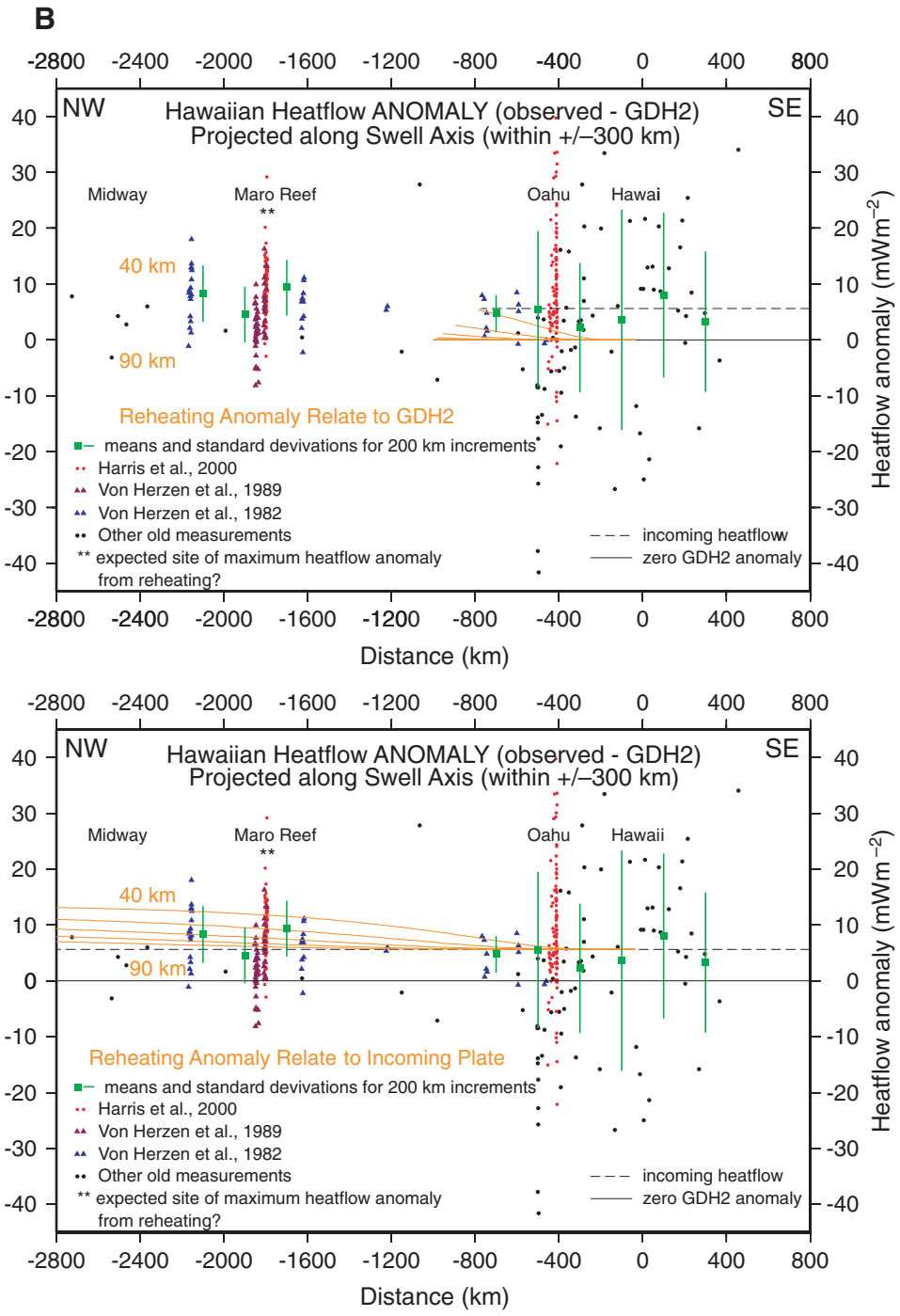

Figure 10. *Continued*

chains is similar to that of the Hawaiian hotspot track. However, the ages of chains do not show the clear progression seen for the Hawaiian chain (Schlanger et al., 1984; Koppers et al., 2003).

The shallow depths and thin effective elastic thicknesses of the lithosphere calculated from the loading of volcanoes and seamounts led McNutt and Fisher (1987) to suggest that the shallow bathymetry resulted from the area lithosphere's having the temperature structure of an anomalously thin 75 km–thick thermal plate. McNutt and Judge (1990) further suggested that the weak flexural strengths, low surface wave velocities (Nishimura and Forsyth, 1985), and geochemical anomalies (Hart, 1984, 1988; Castillo, 1988) were consequences of the combined effects of a thin thermal plate and a deeper low-density plume. In this model the lithosphere is thinned by enhanced heat flux from the mantle and low viscosity beneath the plate such that the weak plate is easily penetrated by hotspot volcanism.

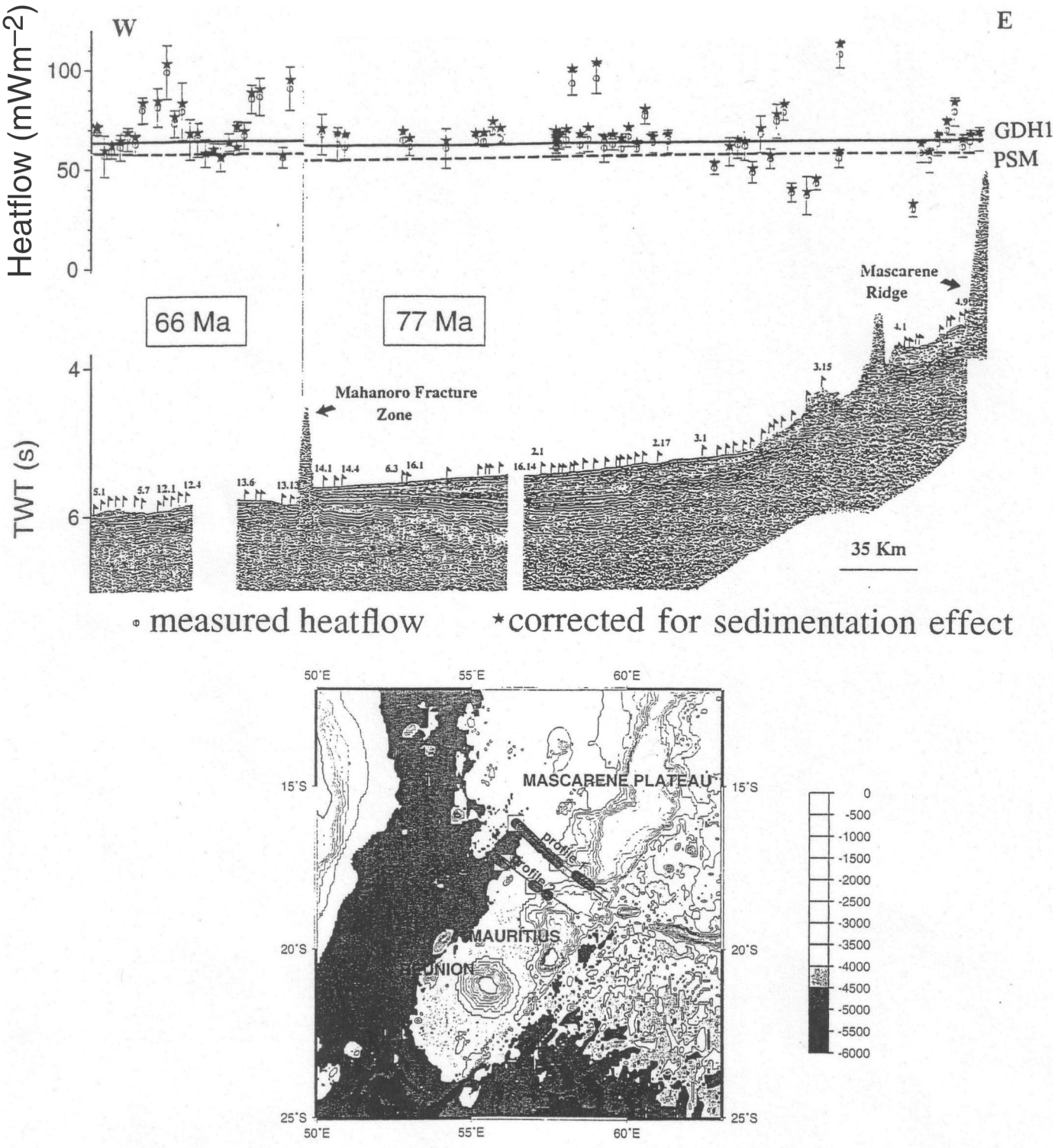

Figure 11. Heatflow across the Réunion swell. The possible anomaly is smaller with respect to GDH1 than is the model of Parsons and Sclater (1977) (PSM) (Bonneville et al., 1997).

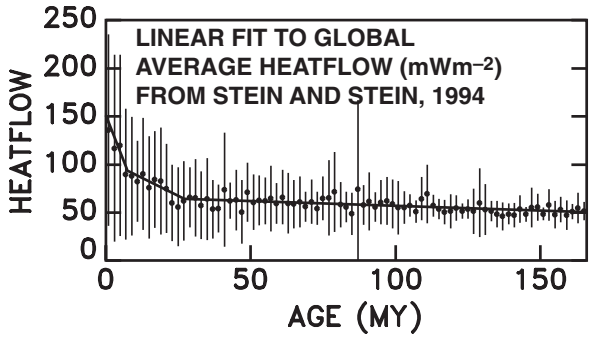

Figure 12. Variations in measured heatflow as a function of age in young lithosphere. Despite the scatter, due in part to hydrothermal circulation, the mean heatflow varies smoothly with age (Stein, 2003).

However, the heatflow data (Fig. 14) rule out the thermal thinning. Although the region is shallower than predicted by GDH1 or sites of comparable age elsewhere in the Pacific, consistent with a thermally thinned plate, the heatflow is no higher than at the other sites or than the global average. However, substantial thinning of the plate predicts heatflow much higher than observed (Stein and Abbott, 1991; Stein and Stein, 1993). Alternative explanations include the dynamic effect of mantle plumes (Sleep, 1992) or the presence of a buoyant volcanic layer just beneath the Moho (McNutt and Bonneville, 2000). The low effective elastic thicknesses may be due to mechanical weakening by the volcanism, intraplate stresses (Stein and Stein, 1993), or an interaction of the flexural effects of volcanoes of different ages (McNutt et al., 1997).

Heatflow also yields insight with regard to the Darwin rise, a large region of shallow bathymetry in the western Pacific that underwent major volcanism and uplift during the Cretaceous. Menard (1984) proposed that the Cretaceous Darwin rise was similar to the present superswell, many of whose hotspot tracks can be traced back to the Darwin rise. McNutt et al. (1990) suggested a schematic history in which the Darwin rise was dynamically uplifted during the Cretaceous and was similar to the present superswell until ca. 70–80 Ma. The present depth was interpreted as anomalously shallow, indicating a residual effect of the transient Cretaceous reheating.

This idea can be excluded, however, because the Darwin rise heatflow data show no evidence for an anomaly relative either to lithosphere of these ages elsewhere in the Pacific or to a thin-plate model (Stein and Abbott, 1991; Stein and Stein, 1993). Similarly, although the depths are anomalously shallow with respect to PSM, they are consistent with a thin plate. Hence we see no evidence for the rise lithosphere's presently retaining a significant thermal signature of the Cretaceous events.

Iceland—On-Ridge Hotspot

Until recently, heatflow has not played much of a role in the debate about hotspots such Iceland, which are on or near mid-ocean ridges, for two reasons. The first is that predictions for heatflow have not been offered, because such hotspots are thought to reflect an interaction between upwelling plumes and nearby spreading centers (Ito et al., 1996), which is more complex than at midplate hotspots, which are generally attributed to a simpler interaction of a plume with a plate interior. Second, seafloor near

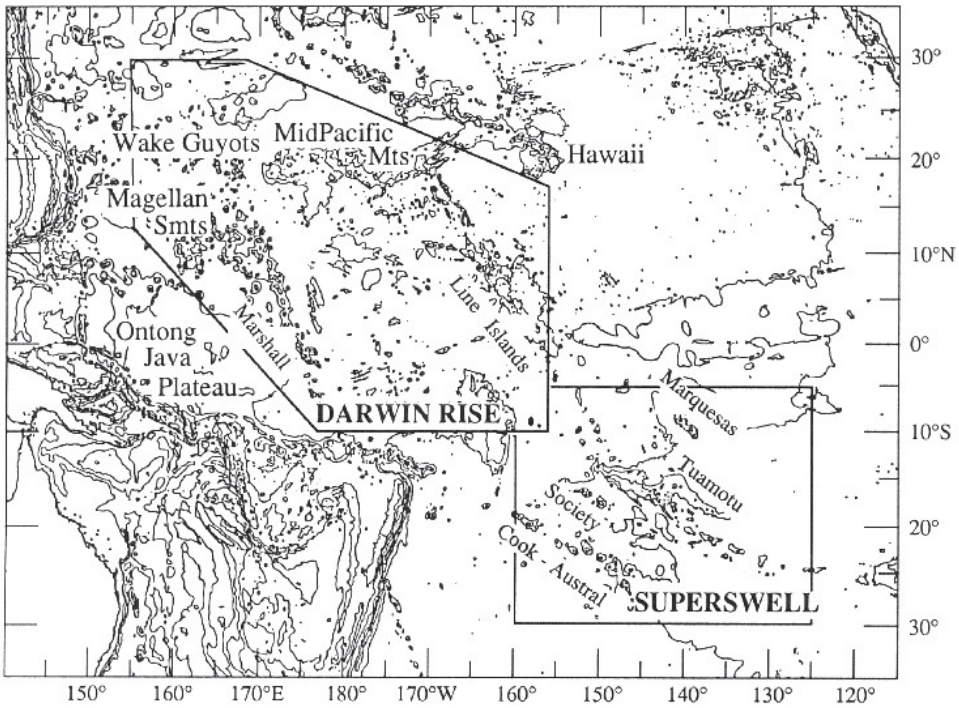

Figure 13. Bathymetry of the Pacific, showing the regions used for Darwin rise and superswell depth and heatflow analyses. Because the extent of the superswell and Darwin rise are ill-defined, the boundaries of the regions used are somewhat arbitrary. From Stein and Stein, 1993.

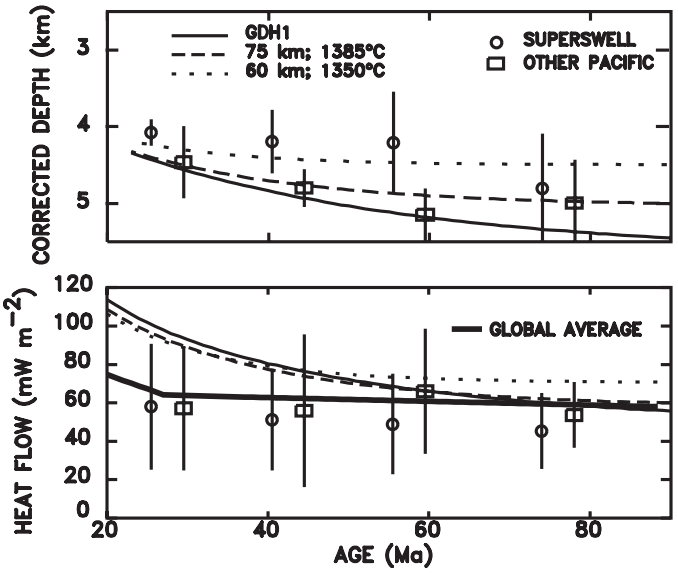

Figure 14. Corrected depth (top) and heatflow (bottom) as a function of age for sites in the superswell and on lithosphere of the same age elsewhere in the Pacific. Data are averaged in 20-m.y. bins. The superswell depths are shallower than the remainder of the Pacific or that expected for GDH1 for ages younger than ca. 70 Ma. Superswell heatflow data do not differ significantly from those for the remainder of the Pacific or from the global average. At ages older than ca. 50 Ma, the data are similar to GDH1 predictions. The heatflow data thus neither require nor exclude the possibility of a thinner thermal lithosphere, as shown by predictions for the 75 km–thick plate with a 1385 °C basal temperature suggested by McNutt and Fisher (1987). The poor fit of the heatflow for ages older than 60 Ma predicted by a 60 km–thick plate argues against further thinning. Modified from Stein and Stein, 1993.

on-ridge hotspots is younger than 40 Ma, so conductive reference models could not effectively be used to characterize "normal" heatflow and assess possible perturbations. As noted, the latter problem can be addressed by using average observed heatflow for lithosphere of the same age elsewhere.

Plume models imply that heatflow should be raised over the "normal" in several ways. The most important is likely to be an indirect effect of plume material migrating along the Mid-Atlantic Ridge (White, 1999). This material should raise temperatures along the ridge by up to several hundred degrees, depending on distance from the plume, so that lithosphere formed at the ridge on either plate would have higher heatflow.

The plume should also have direct effects on heatflow. First, outward-flowing plume material should heat the base of already-formed lithosphere. This effect would be similar to that at Hawaii, but larger because heat is added at the base of the lithosphere, which is thinner near Iceland because of its relative youth. Hence increased heatflow should occur on both sides of the Mid-Atlantic Ridge.

A second direct effect could result from the history of relative motion among the plume, the Mid-Atlantic Ridge, and the two plates. Modeling this history is more complex than modeling that along the Hawaiian-Emperor seamount chain, where the history of volcanism is used to infer the history of the plume. In contrast, the Iceland plume's history cannot be inferred directly from the elevated Iceland-Greenland and Iceland-Faroe plateaus extending westward and eastward from Iceland (Fig. 15), because models assuming various hotspot sizes and motions "offer nonunique solutions that could be used to explain a plateau of any location, origin, and age progression" (Vink, 1984).

To address this ambiguity, Vink (1984) used plate reconstructions assuming that plumes are fixed to predict that the plume presently under Iceland was under Greenland 45 Ma. Since then, westward motion of the Mid-Atlantic Ridge relative to the plume has brought Iceland over the plume. During this time, plume material has flowed laterally beneath the North America plate to the Mid-Atlantic Ridge. The observed trends of the plateaus are matched assuming that plume material flowed to the closest point on the Mid-Atlantic Ridge, where plateaus formed by excess volcanism and were transported away in opposite directions as the two plates spread. Alternatively, White and McKenzie (1989) argued that such lateral flow was not possible. Instead they proposed that a newly formed plume initiated the rifting of the Greenland margin and the opening of the north Atlantic, such that the paired plateaus formed directly above the central plume via ridge jumps that kept the Mid-Atlantic Ridge above the plume's core (White, 1999). Lundin and Doré (this volume) find that only one such ridge jump is apparent in Iceland's history. Although these plume history models differ, and only the first reflects detailed kinematic modeling, we expect that both predict heatflow near Iceland higher on the North America (west) plate than for lithosphere of corresponding age on the Eurasia (east) plate.

We therefore examined (Stein and Stein, 2003) heatflow data for sites within 500 km of Iceland to see if they showed either expected effect—abnormally high heatflow on either side of the ridge and higher heatflow to the west. As shown in Figure 16, we find no evidence for either effect. The North American values, whereby a plume should raise heatflow, are consistent with the global average for lithosphere of that age, including the effect of hydrothermal circulation. Thus if a plume exists, it is not significantly hotter than typical mid-ocean ridges. Moreover, we do observe an asymmetry, but opposite to that expected. To an age of ca. 35 Ma, the European values are generally higher than those for North America, approaching those predicted for the GDH1 model, which does not include hydrothermal effects.

Such striking asymmetry between ridge flanks is unusual. Because the data are sparse, significantly more data will be needed to determine if the asymmetry is real and, if so, to understand it fully. Even so, our sense is that it is likely to be real. We doubt that it is due to thick impermeable sediment that is suppressing hydrothermal circulation (Davis et al., 1992), because this mechanism requires that almost all igneous basement rock be covered, which is not the case here, especially within 10 m.y. of the axis. Moreover, on a global basis sediment thickness rarely has a significant effect on heatflow (Stein et al., 1995).

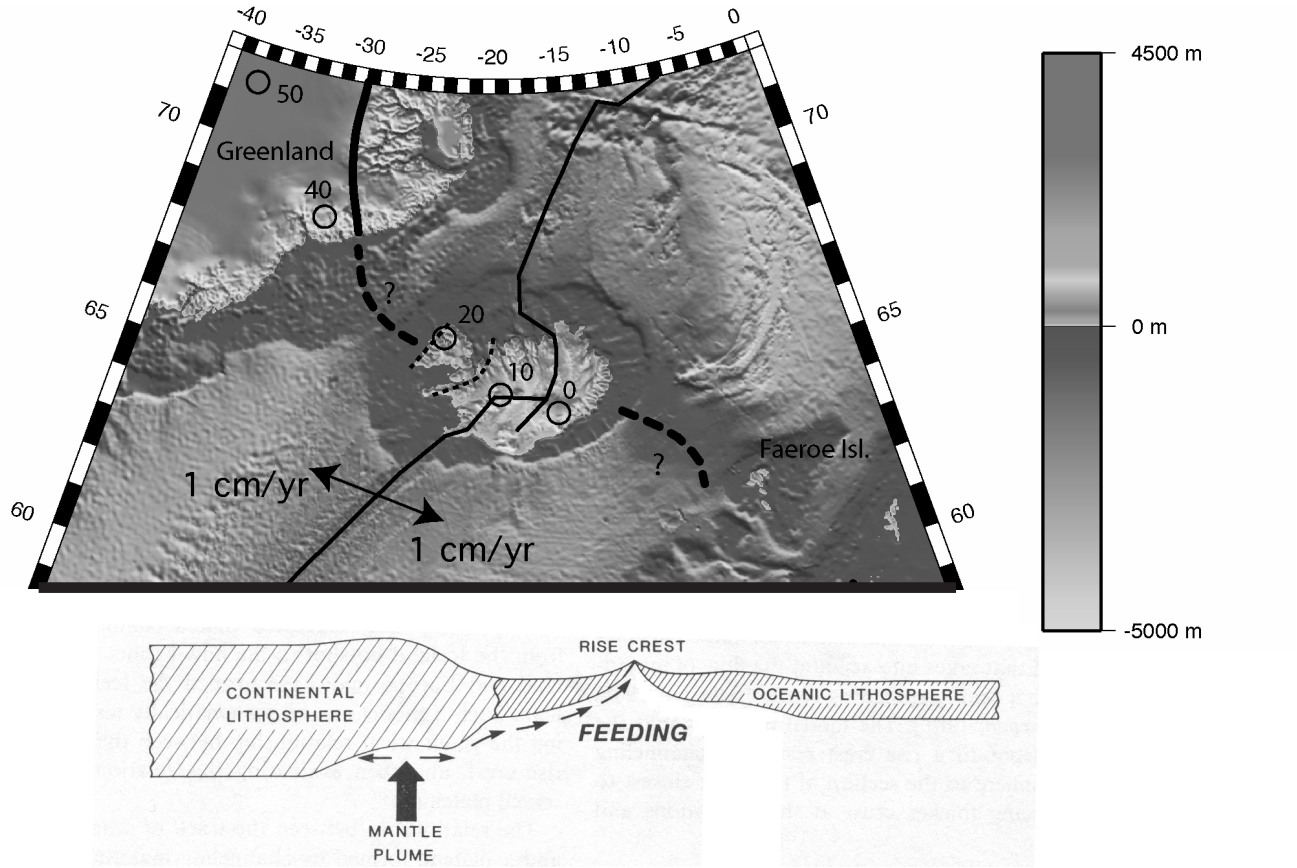

Figure 15. Top: Bathymetric map of the Iceland region showing positions predicted for the hypothesized plume if fixity with other Indo-Atlantic hotspots is assumed (Foulger, 2002). Bottom: Model for plume-ridge interaction (Vink, 1984).

Hence, although sediment effects may contribute, our sense is that they are not the prime cause of the asymmetry.

Instead we suspect that this is a tectonic effect. First, the asymmetry might somehow reflect differences only in mantle temperature between the plates. However, in such a case we expect comparable variations in subsidence, with the hotter Eurasia plate subsiding faster and hence being deeper for a given age. Such an effect has been reported, but the 5% subsidence rate asymmetry (Johansen et al., 1984) is significantly less than that in heatflow. Second, the asymmetry might somehow reflect westward migration (absolute motion) of the Mid-Atlantic Ridge, which may affect spreading processes (Stein et al., 1977; Small and Danyushevsky, 2003). However, initial inspection of data suggests that the asymmetry dies off to the north and south. Third, the asymmetry might reflect ridge migration over an unusual region of the mantle, similar to Foulger's (Foulger, 2002; Foulger et al., this volume) proposal that Iceland results from excess magmatism as the ridge migrates over the Caledonian suture, which contains rocks remaining from an earlier subduction period. In this nonplume model, temperatures are not unusually high but excess melting of more fertile material occurs, consistent with petrologic arguments (Korenaga and Kelemen, 2000). For this to explain the heatflow, the process must generate both higher than normal heatflow and much less anomalous depths.

DISCUSSION

Heatflow data, though not the primary tool used to study midplate swells, yield valuable insights. Although anomalously high heatflow was initially reported for a number of hotspot swells, subsequent analysis shows that most, if not all, of the apparent anomalies resulted from comparing data to thermal models that underestimated heatflow elsewhere. Hence the small or absent heatflow anomalies at hotspots play a role similar to that of the dog whose failure to bark helped Sherlock Holmes locate the missing racehorse Silver Blaze. The present limited data can exclude major effects from hot plumes causing heating of the shallow portions of the lithosphere. However, they cannot discriminate between models that predict only small surface effects, including compositional buoyancy, dynamic uplift, or thermal buoyancy, whose effects are restricted to the lower lithosphere.

Substantially more could be done, however, with better heatflow data. The data are sufficiently sparse that we generally can-

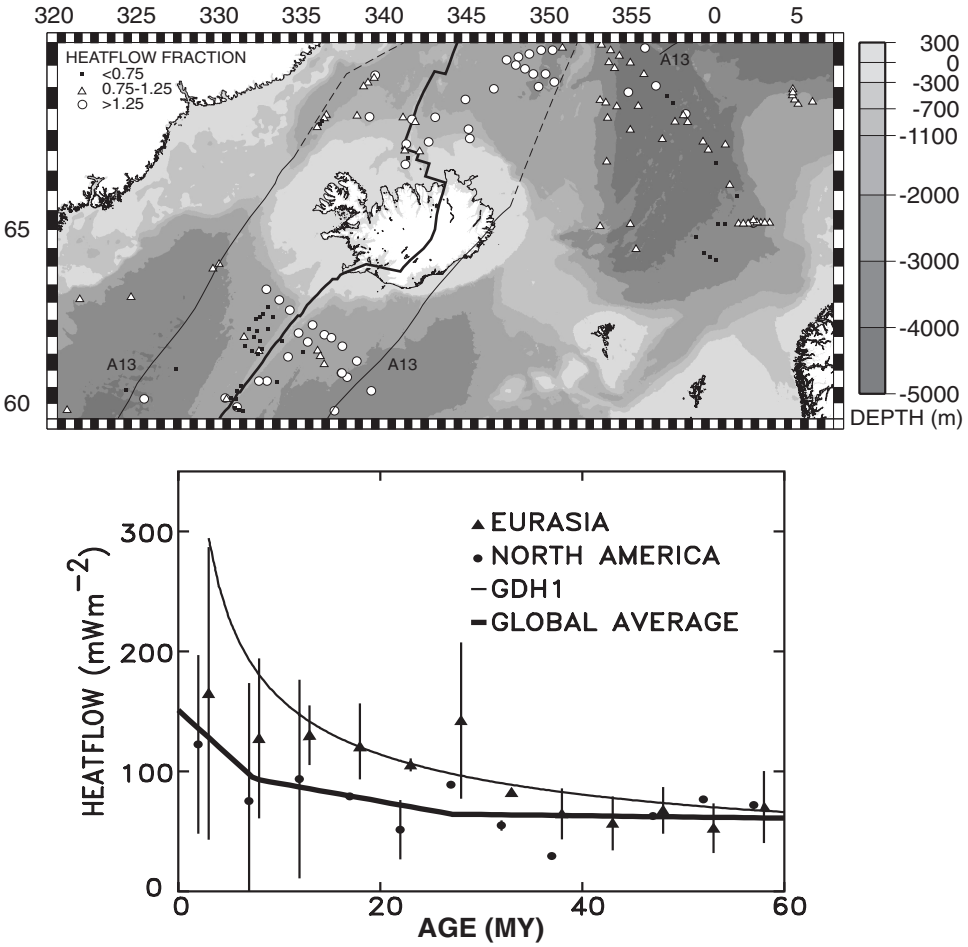

Figure 16. Top: Bathymetry and heatflow for the Iceland region. Heatflow is shown as heatflow fraction, observed values normalized by global average values for that lithospheric age (Fig. 12). Lithosphere younger than ca. 35 Ma is indicated by the positions of magnetic anomaly 13 (solid line) or approximated by the dashed line. Bottom: Heatflow data (from top) grouped in 5 m.y. bins for the Eurasia and North America plates compared to the predictions of the GDH1 thermal model, which does not include the effect of hydrothermal circulation, and a linear fit to the global average values. From Stein and Stein, 2003.

not assess possible spatial patterns or average them well enough to determine if small anomalies are real. Even for Hawaii (Fig. 10) we are working with scattered and poorly sampled data. Hence it is hard to tell whether patterns such as the Iceland regional asymmetry are real or whether an age-dependent signal like that predicted for Hawaii in Figure 9 is present.

This situation has developed largely because in recent years acquisition of marine heatflow data on a global scale has come to a near-standstill. As shown in Figure 17, global heatflow data coverage has improved only slightly since 1982. This situation has developed due to a combination of factors, including the cost of collecting data and a growth of interest in using dense measurements to study hydrothermal systems. If this situation changes, heatflow data should help further advance understanding of the processes causing midplate swells.

Improvement of heatflow data would also allow models to improve beyond their current limits; much of the reason that all four GDH2 variants look similar is the relatively high amount of scatter in the heatflow data. Though using the GTR filter reduced the scatter significantly, the heatflow data still provided the majority of the variance in the final parameters. Similarly, using datasets other than heatflow and bathymetry can provide valuable constraints on the models and may aid in discriminating between two otherwise equally viable alternatives.

However, though improvement of lithospheric cooling models will identify anomalous bathymetry and gravity associated with hotspots and swells with more certainty, and so allow them to be detected more easily, it may not provide the same improvement to anomalous heatflow data. Because hotspot tracks represent a relatively narrow thermal perturbation of the lithosphere, they are unlikely to be visible when looking at global or large regional heatflow anomaly maps. In most such maps, the bin size is large enough that the track-associated heatflow anomaly is smoothed out against the background. Detailed heatflow measurements will be required to determine any anomalies associated with hotspots.

As was the case for Hawaii, gravity data can provide information that conclusively excludes a model. Similarly, the gradient in the GTR shows promise as a method for highlighting anomalous regions. Though we used this technique primarily as a method for excluding "noise" from the model inversion, the excluded regions may form the "signal" for more focused investigations of swell-related processes.

Thus the parameters derived in this paper provide a respite

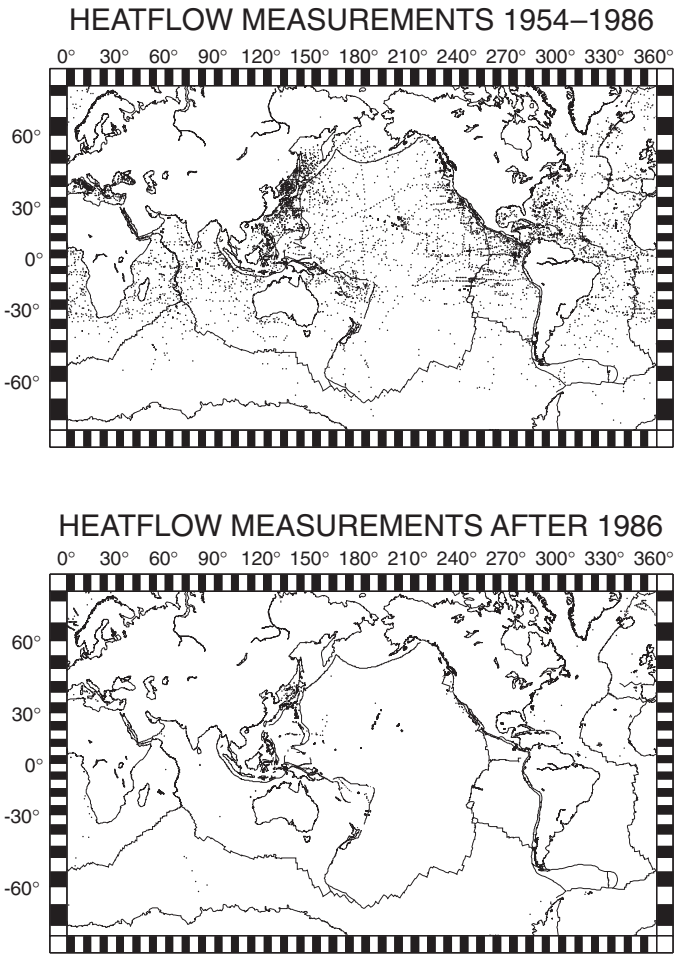

Figure 17. Comparison of marine heatflow data collected before (top) and after (bottom) 1986. Global coverage has not improved greatly in recent years because the focus of such studies has shifted to detailed studies of specific areas.

in the search for a definitive model of lithospheric heatflow, not the final, "absolute" value. The thin-plate models do a better job of determining the observable characteristics of "normal" lithosphere, and so provide a more secure starting point for investigations into "abnormal" regions. As we learn more about these regions, we can expect to once again adjust the models to incorporate our new understanding so that they better reflect the true nature of the processes that underlie both lithospheric cooling and hotspots.

ACKNOWLEDGMENTS

We thank G.R. Foulger, D. Anderson, J. Natland, R. Harris, and an anonymous reviewer for their comments. We thank G. Sella for help and useful advice. This work was supported by National Science Foundation Grant OCE-0001941 to C.A.S.

REFERENCES CITED

Anderson, D.L., 2000, The thermal state of the upper mantle: No room for mantle plumes: Geophysical Research Letters, v. 27, p. 3623–3626, doi: 10.1029/2000GL011533.

Bijwaard, H., and Spakman, W., 1999, Tomographic evidence for a narrow whole mantle plume beneath Iceland: Earth and Planetary Science Letters, v. 166, p. 121–126, doi: 10.1016/S0012-821X(99)00004-7.

Bonneville, A., Von Herzen, R.P., and Lucazeau, F., 1997, Heat flow over Réunion hot spot track: Additional evidence for thermal rejuvenation of oceanic lithosphere: Journal of Geophysical Research, v. 102, p. 22,731–22,747, doi: 10.1029/97JB00952.

Buck, W.R., and Parmentier, E.M., 1986, Convection beneath young oceanic lithosphere: Implications for thermal structure and gravity: Journal of Geophysical Research, v. 91, p. 1961–1974.

Castillo, P., 1988, The Dupal anomaly as a trace of the upwelling lower mantle: Nature, v. 336, p. 667–670, doi: 10.1038/336667a0.

Cazenave, A., 1984, Thermal cooling of the lithosphere: New constraints from geoid height data: Earth and Planetary Science Letters, v. 70, p. 395–406, doi: 10.1016/0012-821X(84)90023-2.

Christiansen, R.L., Foulger, G.R., and Evans, J.R., 2002, Upper-mantle origin of the Yellowstone hotspot: Geological Society of America Bulletin, v. 114, p. 1245–1256, doi: 10.1130/0016-7606(2002)1142.0.CO;2.

Clague, D.A., Moore, J.G., Dixon, J.E., and Friesen, W.B., 1995, Petrology of submarine labs from Kilauea's Puna Ridge, Hawaii: Journal of Petrology, v. 36, p. 299–349.

Cochran, J.R., and Buck, W.R., 2001, Near-axis subsidence rates, hydrothermal circulation, and thermal structure of mid-ocean ridge crests: Journal of Geophysical Research, v. 106, p. 19,233–19,258, doi: 10.1029/2001JB000379.

Crough, S.T., 1977, Approximate solutions for the formation of the lithosphere: Physics of the Earth and Planetary Interiors, v. 14, p. 365–377, doi: 10.1016/0031-9201(77)90169-8.

Crough, S.T., 1978, Thermal origin of mid-plate hot-spot swells: Geophysical Journal of the Royal Astronomical Society, v. 55, p. 451–469.

Crough, S.T., 1983, Hotspot swells: Annual Reviews of Earth and Planetary Sciences, v. 11, p. 165–193, doi: 10.1146/annurev.ea.11.050183.001121.

Davies, G.F., 1988, Ocean bathymetry and mantle convection, 1: Large-scale flow and hotspots: Journal of Geophysical Research, v. 93, p. 10,467–10,480.

Davis, E.E., and Lister, C.R.B., 1974, Fundamentals of ridge crest topography, Earth and Planetary Science Letters, v. 21, p, 405–413.

Davis, E.E., Chapman, D.S., Mottl, M.J., Bentkowski, W.J., Dadey, K., Forster, C., Harris, R., Nagihara, S., Rohr, K., Wheat, G., and Whiticar, M., 1992, FlankFlux: An experiment to study the nature of hydrothermal circulation in young oceanic crust: Canadian Journal of Earth Sciences, v. 29, p. 925–952.

DeLaughter, J., Stein, S., and Stein, C., 1999, Extraction of the lithospheric aging signal from satellite geoid data: Earth and Planetary Science Letters, v. 174, p. 173–181, doi: 10.1016/S0012-821X(99)00247-2.

DeLaughter, J.E., 1998, Evolution of the lithospheres of earth and Venus: Studies in geoid topography and heat flow [Ph.D. dissertation]: Evanston, Illinois, USA: Northwestern University.

DePaolo, D., and Manga, M., 2003, Deep origin of hotspots: The mantle plume model: Science, v. 300, p. 920–921, doi: 10.1126/science.1083623.

Divins, D., 2004, Total sediment thickness of the world's oceans and marginal seas: Boulder, Colorado: World Data Center for Marine Geology and Geophysics, http://www.ngdc.noaa.gov/mgg/sedthick/sedthick.html, February.

Doin, M.P., and Fleitout, L., 1996, Thermal evolution of the oceanic lithosphere: An alternative view: Earth and Planetary Science Letters, v. 142, p. 121–136, doi: 10.1016/0012-821X(96)00082-9.

Duncan, R.A., and Clague, D.A., 1985, Pacific plate motion recorded by linear volcanic chains, *in* Nairn, A.E., et al., eds., The ocean basins and margins, vol. 7A: The Pacific Ocean: New York, Plenum Press, p. 89–121.

Foulger, G.R., 2002, Plumes or plate tectonic processes?: Astronomy and Geophysics, v. 43, p. 19–23.

Foulger, G.R., and Natland, J., 2003, Is "hotspot" volcanism a consequence of plate tectonics: Science, v. 300, p. 921–922, doi: 10.1126/science.1083376.

Foulger, G.R., Pritchard, M.J., Julian, B.R., Evans, J.R., Allen, R.M., Nolet, G., Morgan, W.J., Bergsson, B.H., Elendsson, P., Jakobsdottir, S., Ragnarsson, S., Stefansson, R., and Vogfjordd, K., 2001, Seismic tomography shows that upwelling beneath Iceland is confined to the upper mantle: Geophysical Journal International, v. 146, p. 504–530, doi: 10.1046/j.0956-540x.2001.01470.x.

Hager, B.H., and O'Connell, R.J., 1980, Lithospheric thickening and subduction, plate motions and mantle convection, *in* Dziewonski, A.M., and Boschi, E., eds., Physics of the Earth's interior: Proceedings of the International School of Physics, "Enrico Fermi": Amsterdam, North-Holland Publishing Co., p. 464–492.

Hamilton, W., 2002, The closed upper-mantle circulation of plate tectonics, *in* Stein, S., and Freymueller, J., eds., Plate boundary zones: Washington, D.C., American Geophysical Union, p. 359–410.

Harris, R.N., Von Herzen, R.P., McNutt, M.K., Garven, G., and Jordahl, K., 2000a, Submarine hydrogeology of the Hawaiian archipelagic apron, 1: Heat flow patterns north of Oahu and Maro Reef: Journal of Geophysical Research, v. 105, p. 21,353–21,369, doi: 10.1029/2000JB900165.

Harris, R.N., Garven, G., Georgen, J., McNutt, M.K., Christiansen, L., and Von Herzen, R.P., 2000b, Submarine hydrogeology of the Hawaiian archipelagic apron, 2: Numerical simulations of coupled heat transport and fluid flow: Journal of Geophysical Research, v. 105, p. 21,371–21,385, doi: 10.1029/2000JB900164.

Hart, S.R., 1984, A large-scale isotope anomaly in the Southern Hemisphere mantle: Nature, v. 309, p. 753–757, doi: 10.1038/309753a0.

Hart, S.R., 1988, Heterogeneous mantle domains: Signatures, genesis and mixing chronologies: Earth and Planetary Science Letters, v. 90, p. 273–296, doi: 10.1016/0012-821X(88)90131-8.

Hegel, G.W.F., 1816, Wissenschaft der Logik: Zweiter Band Die subjektive Logik: Nürnberg, Germany.

Humphreys, E.D., Dueker, K.G., Schutt, D.L., and Smith, R.B., 2000, Beneath Yellowstone: Evaluating plume and nonplume models using teleseismic images of the upper mantle: GSA Today, v. 10, p. 1–7.

Ito, G., Lin, J., and Gable, C.W., 1996, Dynamics of mantle flow and melting at a ridge-centered hotspot: Earth and Planetary Science Letters, v. 144, p. 53–74, doi: 10.1016/0012-821X(96)00151-3.

Jackson, E.D., and Shaw, H.R., 1975, Stress fields in central portions of the Pacific plate: Delineated in time by linear volcanic chains: Journal of Geophysical Research, v. 80, p. 1861–1874.

Jarvis, G.T., and Peltier, W.R., 1989, Convection models and geophysical observations, *in* Peltier, W.R., ed., Mantle convection: New York, Gordon and Breach, p. 479–594.

Johansen, B., Vogt, P.R., and Eldholm, O., 1984, Reykjanes ridge: Further analysis of crustal subsidence and time-transgressive basement topography: Earth and Planetary Science Letters, v. 68, p. 249–258, doi: 10.1016/0012-821X(84)90157-2.

Kido, M., and Seno, T., 1994, Dynamic topography compared with residual depth anomalies in oceans and implications for age-depth curves: Geophysical Research Letters, v. 21, p. 717–720, doi: 10.1029/94GL00305.

King, S.D., and Anderson, D.L., 1998, Edge-driven convection, 5: Earth and Planetary Science Letters, v. 160, p. 289–296, doi: 10.1016/S0012-821X(98)00089-2.

Koppers, A.A.P., Staudigal, H., Pringle, M.S., and Wijbrans, J.R., 2003, Short-lived and discontinuous intraplate volcanism in the South Pacific: Hot spots or extensional volcanism?: Geochemistry, Geophysics, Geosystems, v. 4, doi:10.1029/2003GC000533.

Korenaga, J., and Kelemen, P.B., 2000, Major element heterogeneity in the mantle source of the North Atlantic igneous province: Earth and Planetary Science Letters, v. 184, p. 251–268, doi: 10.1016/S0012-821X(00)00308-3.

Langseth, M.G., Le Pichon, X., and Ewing, M., 1966, Crustal structure of the mid-ocean ridges, V: Heat flow through the Atlantic Ocean floor and convection currents: Journal of Geophysical Research, v. 71, p. 5321–5355.

Larson, R.L., 1991, Geological consequences of superplumes: Geology, v. 19, p. 963–966, doi: 10.1130/0091-7613(1991)0192.3.CO;2.

Li, X., Kind, R., Yuan, X., Wolbern, I., and Hanka, W., 2004, Rejuvenation of the lithosphere by the Hawaiian plume: Nature, v. 427, p. 827–829, doi: 10.1038/nature02349.

Liu, M., and Chase, C.G., 1989, Evolution of midplate hotspot swells: Numerical solutions: Journal of Geophysical Research, v. 94, p. 5571–5584.

McKenzie, D.P., 1967, Some remarks on heat flow and gravity anomalies: Journal of Geophysical Research, v. 72, p. 6261–6273.

McNutt, M., and Bonneville, A., 2000, A shallow, chemical origin for the Marquesas swell: Geochemistry, Geophysics, Geosystems., v. 1, 1999GC00028.

McNutt, M., Caress, D., Reynolds, J., Jordahl, K.A., and Duncan, R.A., 1997, Failure of plume theory to explain midplate volcanism in the southern Austral Islands: Nature, v. 389, p. 479–482, doi: 10.1038/39013.

McNutt, M.K., 2002, Heat flow variations over Hawaiian swell controlled by near-surface processes, not plume properties, *in* Takahashi, E., et al., eds., Hawaiian volcanoes: Deep underwater perspectives: Washington, D.C., American Geophysical Union, Geophysical Monograph 128, p. 365–372.

McNutt, M.K., and Fisher, K.M., 1987, The South Pacific superswell, *in* Keating, B.H., et al., eds., Seamounts, islands, and atolls: Washington, D.C., American Geophysical Union, Geophysical Monograph 43, p. 25–34.

McNutt, M.K., and Judge, A.V., 1990, The superswell and mantle dynamics beneath the South Pacific: Science, v. 248, p. 969–975.

McNutt, M.K., Winterer, E.L., Sager, W.W., Natland, J.H., and Ito, G., 1990, The Darwin rise: A Cretaceous superswell?: Geophysical Research Letters, v. 17, p. 1101–1104.

Menard, H.W., 1969, Elevation and subsidence of oceanic crust: Earth and Planetary Science Letters, v. 6, p. 275–284, doi: 10.1016/0012-821X(69)90168-X.

Menard, H.W., 1984, Darwin reprise: Journal of Geophysical Research, v. 89, p. 9960–9968.

Montelli, R., Nolet, G., Dahlen, F.A., Masters, G., Engdahl, E.R., and Hung, S.-H., 2004, Finite-frequency tomography reveals a variety of plumes in the mantle: Science, v. 303, p. 338–343, doi: 10.1126/science.1092485.

Morgan, W.J., 1971, Convection plumes in the lower mantle: Nature, v. 230, p. 42–43.

Mueller, R.D., Roest, W.R., Royer, J.-Y., Gahagan, L.M., and Sclater, J.G., 1997, Digital isochrons of the world's ocean floor: Journal of Geophysical Research, v. 102, p. 3211–3214, doi: 10.1029/96JB01781.

Nerem, R.S., Lerch, F.J., Williamson, R.G., Klosko, S.M., Robbins, J.W., and Patel, G.B., 1994, Gravity model improvements using the DORIS tracking system on the SPOT2 satellite: Journal of Geophysical Research, v. 99, p. 2791–2813, doi: 10.1029/93JB02567.

Nishimura, C.E., and Forsyth, D.W., 1985, Anomalous Love-wave phase velocities in the Pacific: Sequential pure-path and spherical harmonic inversion: Geophysical Journal of the Royal Astronomical Society, v. 81, p. 389–407.

Norton, I.O., 1995, Plate motions in the North Pacific: The 43 Ma nonevent: Tectonics, v. 14, p. 1080–1094, doi: 10.1029/95TC01256.

Parsons, B., and McKenzie, D.P., 1978, Mantle convection and the thermal structure of the plates: Journal of Geophysical Research, v. 83, p. 4485–4496.

Parsons, B., and Sclater, J.G., 1977, An analysis of the variation of ocean floor bathymetry and heat flow with age: Journal of Geophysical Research, v. 82, p. 803–827.

Popper, K., 1935, Logik der Forschung: Vienna, Julius Springer Verlag.

Richardson, W.P., Stein, S., Stein, C., and Zuber, M.T., 1995, Geoid data and the thermal structure of the oceanic lithosphere: Geophysical Research Letters, v. 22, p. 1913–1916, doi: 10.1029/95GL01595.

Robinson, E.M., 1988, The topographic and gravitational expression of density anomalies due to melt extraction in the uppermost oceanic mantle: Earth

and Planetary Science Letters, v. 90, p. 221–228, doi: 10.1016/0012-821X(88)90102-1.

Schlanger, S.O., Garcia, M.O., Keating, B.H., Naughton, J.J., Sager, W.W., Haggerty, J.A., Philpotts, J.A., and Duncan, R.A., 1984, Geology and geochronology of the Line Islands: Journal of Geophysical Research, v. 89, p. 11,261–11,272.

Shen, Y., Solomon, S.C., Bjarnson, I., Nolet, G., Morgan, W.J., Allen, R.M., Vogfjord, K., Jakobsdottir, S., Stefansson, R., Julian, B.R., and Foulger, G.R., 2002, Seismic evidence for a tilted mantle plume and north-south mantle flow beneath Iceland: Earth and Planetary Science Letters, v. 197, p. 261–272, doi: 10.1016/S0012-821X(02)00494-6.

Shoberg, T., Stein, C., and Stein, S., 1993, Constraints on lithospheric thermal structure for the Indian Ocean from depth and heat flow data: Geophysical Research Letters, v. 20, p. 1095–1098.

Sleep, N.H., 1990, Hot spots and mantle plumes: Some phenomenology: Journal of Geophysical Research, v. 95, p. 6715–6736.

Sleep, N.H., 1992, Hotspots and mantle plumes: Annual Reviews of Earth and Planetary Sciences, v. 20, p. 19–43, doi: 10.1146/annurev.ea.20.050192.000315.

Sleep, N.H., 1994, Lithospheric thinning by midplate mantle plumes and the thermal history of hot plume material ponded and sublithospheric depths: Journal of Geophysical Research, v. 99, p. 9327–9343, doi: 10.1029/94JB00240.

Sleep, N.H., 2003, Mantle plumes?: Astronomy and Geophysics, v. 44, p. 11–12.

Small, C., and Danyushevsky, L., 2003, A plate kinematic explanation for mid-ocean ridge depth discontinuities: Geology, v. 31, no. 5, p. 399–402.

Smith, W.H.F., and Sandwell, D.T., 1997, Global seafloor topography from satellite altimetry and ship depth soundings: Science, v. 277, p. 1956–1962, doi: 10.1126/science.277.5334.1956.

Stein, C., and Abbott, D., 1991, Heat flow constraints on the South Pacific superswell: Journal of Geophysical Research, v. 96, p. 16,083–16,100.

Stein, C., and Stein, S., 2003, Mantle plumes: Heat flow near Iceland: Astronomy and Geophysics, v. 44, p. 8–10.

Stein, C.A., 2003, Heat flow and flexure at subduction zones: Geophysical Research Letters, v. 30, doi: 10.1029/2003GL018478.

Stein, C.A., and Stein, S., 1992, A model for the global variation in oceanic depth and heat flow with lithospheric age: Nature, v. 359, p. 123–129, doi: 10.1038/359123a0.

Stein, C.A., and Stein, S., 1993, Constraints on Pacific midplate swells from global depth-age and heat flow–age models, *in* Pringle, M., et al., eds., The Mesozoic Pacific: Washington, D.C., American Geophysical Union, Geophysical Monograph 77, p. 53–76.

Stein, C.A., and Stein, S., 1994, Constraints on hydrothermal heat flux through the oceanic lithosphere from global heat flow: Journal of Geophysical Research, v. 99, p. 3081–3095, doi: 10.1029/93JB02222.

Stein, C.A., Stein, S., and Pelayo, A.M., 1995, Heat flow and hydrothermal circulation, *in* Humphris, S., et al., eds., Seafloor hydrothermal systems: Physical, chemical, biological, and geological interactions: Washington, D.C., American Geophysical Union, Geophysical Monograph 91, p. 425–445.

Stein, S., and Stein, C., 1997, Ocean depths and the Lake Wobegon effect: Science, v. 275, p. 1613–1614.

Stein, S., Melosh, H.J., and Minster, J.B., 1977, Ridge migration and asymmetric sea-floor spreading: Earth and Planetary Science Letters, v. 36, p. 51–62, doi: 10.1016/0012-821X(77)90187-X.

Tarduno, J.A., Duncan, R.A., Scholl, D.W., Cottrell, R.D., Steinberger, B., Thordarson, T., Kerr, B.C., Neal, C.R., Frey, F.A., Torii, M., and Carvallo, C., 2003, The Emperor seamounts: Southward motion of the Hawaiian hotspot plume in earth's mantle: Science, v. 301, p. 1064–1069.

Van Ark, E., and Lin, J., 2004, Time variation in hotspot fluxes and isostatic compensation of the Hawaiian-Emperor seamount chain in the Pacific ocean: Journal of Geophysical Research, v. 109, doi: 1Q.1029/2003JB002949..

Vink, G.E., 1984, A hotspot model for Iceland and the Voring plateau: Journal of Geophysical Research, v. 89, p. 9949–9959.

Vogt, P.R., 1981, On the applicability of thermal conduction models to mid-plate volcanism: Comments on a paper by Gass et al., Journal of Geophysical Research, v. 86, p. 950–960.

Von Herzen, R.P., Detrick, R.S., Crough, S.T., Epp, D., and Fehn, U., 1982, Thermal origin of the Hawaiian swell: Heat flow evidence and thermal models: Journal of Geophysical Research, v. 87, p. 6711–6723.

Von Herzen, R.P., Cordery, M.J., Detrick, R.S., and Fang, C., 1989, Heat flow and the thermal origin of hotspot swells: The Hawaiian swell revisited: Journal of Geophysical Research, v. 94, p. 13,783–13,799.

Wessel, P., 1993, A reexamination of the flexural deformation beneath the Hawaiian Islands: Journal of Geophysical Research, v. 98, p. 12,177–12,190.

White, R.S., 1999, Rift-plume interaction in the North Atlantic, *in* Cann, J.R., et al., eds., Mid-ocean ridges" Cambridge, England: Cambridge University Press, p. 103–123.

White, R.S., and McKenzie, D., 1989, Magmatism at rift zones: The generation of volcanic continental margins and flood basalts: Journal of Geophysical Research, v. 94, p. 7685–7729.

Woods, M.T., Leveque, J.-J., Okal, E.A., and Cara, M., 1991, Two-station measurements of Rayleigh wave group velocity along the Hawai'ian swell: Geophysical Research Letters, v. 18, p. 105–108.

Manuscript Accepted by the Society January 3, 2005

Printed in the USA